NAVAL POSTGRADUATE SCHOOL

MONTEREY, CALIFORNIA

THESIS

PRELIMINARY DESIGN STUDY OF AN ENHANCED
MIXING EDUCTOR SYSTEM FOR THE LHA (R) GAS
TURBINE EXHAUST

by

Stephen W. Dudar

December 2003

Thesis Advisor: Knox T. Millsaps, Jr.

Approved for public release, distribution unlimited

THIS PAGE INTENTIONALLY LEFT BLANK

REPORT DOCUMENTATION PAGE		*Form Approved OMB No. 0704-0188*
Public reporting burden for this collection of information is estimated to average 1 hour per response, including the time for reviewing instruction, searching existing data sources, gathering and maintaining the data needed, and completing and reviewing the collection of information. Send comments regarding this burden estimate or any other aspect of this collection of information, including suggestions for reducing this burden, to Washington headquarters Services, Directorate for Information Operations and Reports, 1215 Jefferson Davis Highway, Suite 1204, Arlington, VA 22202-4302, and to the Office of Management and Budget, Paperwork Reduction Project (0704-0188) Washington DC 20503.		
1. AGENCY USE ONLY *(Leave blank)*	**2. REPORT DATE** December 2003	**3. REPORT TYPE AND DATES COVERED** Master's Thesis
4. TITLE AND SUBTITLE: Preliminary Design Study Of An Enhanced Mixing Eductor System For The LHA (R) Gas Turbine Exhaust		**5. FUNDING NUMBERS**
6. AUTHOR(S) Stephen W. Dudar		
7. PERFORMING ORGANIZATION NAME(S) AND ADDRESS(ES) Naval Postgraduate School Monterey, CA 93943-5000		**8. PERFORMING ORGANIZATION REPORT NUMBER**
9. SPONSORING /MONITORING AGENCY NAME(S) AND ADDRESS(ES) N/A		**10. SPONSORING/MONITORING AGENCY REPORT NUMBER**
11. SUPPLEMENTARY NOTES The views expressed in this thesis are those of the author and do not reflect the official policy or position of the Department of Defense or the U.S. Government.		
12a. DISTRIBUTION / AVAILABILITY STATEMENT Approved for public release, distribution unlimited		**12b. DISTRIBUTION CODE** A
13. ABSTRACT (maximum 200 words) A preliminary design study was conducted to determine the geometry for an enhanced mixing eductor system for the Landing, Helicopter Assault Ship Replacement (LHA R) program gas turbine exhaust. A one-dimensional analytical model, with a correction factor applied to the secondary mass flow, was developed to predict the secondary air mass flow rate and the exhaust temperature at the mixing tube exit plane. The resultant design consisted of a high aspect ratio lobed nozzle and a mixing tube. The model was also used to predict the backpressure developed by the ducting configuration. The proposed design resulted in a 50% reduction in exhaust temperature with only a 6 inch H_2O increase in back pressure. A detailed design of the oval-to-rectangular transition duct is provided, based on empirical data from a similar duct design. The study also included a prediction of plume radiation intensity in the 3-5 μm band for various aspect ratio slots.		
14. SUBJECT TERMS Eductor, Enhanced Mixing, Lobed Mixer, Gas Turbine Exhaust, Plume Radiation, Oval-to-Rectangular Transition		**15. NUMBER OF PAGES** 79
		16. PRICE CODE
17. SECURITY CLASSIFICATION OF REPORT Unclassified	**18. SECURITY CLASSIFICATION OF THIS PAGE** Unclassified	**19. SECURITY CLASSIFICATION OF ABSTRACT** Unclassified	**20. LIMITATION OF ABSTRACT** UL

THIS PAGE INTENTIONALLY LEFT BLANK

PRELIMINARY DESIGN STUDY OF AN ENHANCED MIXING EDUCTOR
SYSTEM FOR THE LHA (R) GAS TURBINE EXHAUST

Stephen W. Dudar
Lieutenant Commander, United States Navy
B.S.M.E., Virginia Military Institute, 1991

Submitted in partial fulfillment of the
requirements for the degree of

MASTER OF SCIENCE IN MECHANICAL ENGINEERING

from the

NAVAL POSTGRADUATE SCHOOL
December 2003

Author: Stephen W. Dudar

Approved by: Knox T. Millsaps, Jr.
                   Thesis Advisor

                   Anthony J. Healey
                   Chairman, Department of Mechanical and Astronautical
                   Engineering

THIS PAGE INTENTIONALLY LEFT BLANK

ABSTRACT

A preliminary design study was conducted to determine the geometry for an enhanced mixing eductor system for the Landing, Helicopter Assault Ship Replacement (LHA (R)) program gas turbine exhaust. A one-dimensional analytical model, with a correction factor applied to the secondary mass flow, was developed to predict the secondary air mass flow rate and the exhaust temperature at the mixing tube exit plane. The resultant design consisted of a high aspect ratio lobed nozzle and a mixing tube. The model was also used to predict the backpressure developed by the ducting configuration. The proposed design resulted in a 50% reduction in exhaust temperature with only a 6 inch H_2O increase in backpressure. A detailed design of the oval-to-rectangular transition duct is provided, based on empirical data from a similar duct design. The study also included a prediction of plume radiation intensity in the 3-5 μm band for various aspect ratio slots.

THIS PAGE INTENTIONALLY LEFT BLANK

TABLE OF CONTENTS

THIS PAGE INTENTIONALLY LEFT BLANK

LIST OF FIGURES

NOMENCLATURE

DESIGN STUDY

Symbols	Description	Units
A	Cross-sectional area	$[m^2]$ or $[ft^2]$
D_h	Hydraulic diameter	[m] or [ft]
f	Friction factor	[1]
g	Acceleration due to gravity	$[m/s^2]$ or $[ft/s^2]$
H	Head loss	[m] or [ft]
$\dot{m}$	Mass flow rate	[kg/s] or [lbm/s]
P	Pressure	[Pa] or [psi]
R	Gas constant	[J/kg-K] or [Btu/lbm-R]
SG	Specific Gravity	[1]
T	Temperature	[K] or [R]
V	Velocity	[m/s] or [ft/s]
$W = \dfrac{\dot{m}_{secondary}}{\dot{m}_{primary}}$	Pumping ratio	[1]
Z	Distance	[m] or [ft]

Greek Symbols	Description	Units
ρ	Density	$[kg/m^3]$ or $[lbm/ft^3]$
γ	Ratio of specific heats	[1]
$\zeta = \dfrac{(P_{t1} - P_{t2})}{\frac{1}{2}\rho V^2}$	Total pressure loss coefficient	[1]

Subscripts	Description
a	Exhaust duct inlet
atm	Ambient conditions
corr	Mass flow corrected

e	Mixing tube exit	
ref	Reference	
t	Total (Stagnation)	
1	Transition duct inlet	
2	Nozzle inlet	
3	Nozzle exit	
4	Secondary flow inlet	

PLUME RADIATION STUDY

Symbols	Description	Units
A	Total band absorbtance	$[cm^{-1}]$
b	Pressure parameter	[1]
E	Emissive power	$[W/m^2\text{-sr}]$
f	Fuel-to-air ratio	[1]
I	Intensity	$[W/m^2\text{-sr}]$
$\dot{m}$	Mass flow rate	[lbm/s]
n	Pressure parameter	[1]
P_e	Effective pressure	[1]
P_s	Shaft horse power	[hp]
p	Pressure	[atm]
s	Path length	[m]
SFC	Specific Fuel Consumption	[lbm/hp-hr]
X	Pressure path length	$[g/m^2]$
Greek Symbols	Description	Units
α	Band strength parameter	$[cm^{-1}/(g/m^2)]$
β	Line overlap parameter	[1]
γ	Band overlap parameter	[1]
ε	Emissivity	[1]
η	Wave number	$[cm^{-1}]$
ρ_a	Gas density	$[g/m^3]$

$\sigma = 5.67 \times 10^{-8}$ Stefan-Boltzmann constant $[W/m^2\text{-}K^4]$

τ_o Gas band optical thickness   [1]

ω Band width parameter $[cm^{-1}]$

<u>Subscripts</u>	<u>Description</u>
a	Ambient conditions
b	Black body
e	Mixing tube exit
o	Reference

THIS PAGE INTENTIONALLY LEFT BLANK

I. INTRODUCTION

A. MOTIVATION

The search for a more efficient propulsion plant that meets or exceeds current capability, while reducing maintenance requirements has led the United States Navy to investigate an all-electric ship. A first step on the road to the all-electric ship is a modification to the WASP class Landing, Helicopter and Docking Assault ship (LHD), Reference [1]. The eighth ship of the WASP class (LHD 8) is to incorporate a hybrid gas turbine and electric motor for propulsion into the existing hull and superstructure of the LHD 1. The WASP class (LHD 1 through LHD 7) propulsion plant consists of two 600 psi boilers and two 35,000 hp steam turbines that can propel the 40,500 ton Amphibious Assault Ship at 25 knots. In order to meet the Horsepower requirements of the LHD 8, the General Electric LM2500+ was chosen to replace the steam plant along with a 5,000 hp auxiliary propulsion motor that will be used for loitering on station. The Landing, Helicopter Assault Ship Replacement (LHA (R)) program will be the follow-on to the aging WASP class, and is to have the same propulsion plant and similar hull form as the LHD 8 with improvements in superstructure design in order to reduce radar cross section.

There are many advantages to using gas turbines for propulsion. Some advantages include, improved power-to-weight ratio, reduced maintenance requirements, and reduced engineering watch stander requirements. However, the temperature of the gas turbine exhaust can be in excess of 1000 ^{o}F (800 K), roughly 500 ^{o}F (530 K) higher than a conventional steam plant. The increased temperature can damage electronic equipment mounted on the mast as the hot exhaust plume comes in contact with it. Additionally, the ship surfaces which normally radiate as nearly a black body in the 8-14 μm band are heated after coming in contact with the plume, and now radiate at a higher intensity given by $I=(\varepsilon\sigma T^4)/\pi$ (where T is the exhaust temperature in Kelvin, ε is the emissivity and $\sigma=5.67\times10^{-8}$ is the Stefan-Boltzmann constant), Figure [1].

Since the intensity of the plume also goes as T^4, the intensity of gas turbine exhaust can be 16 times greater than the conventional steam plant. The two main byproducts of combustion, CO_2 and H_2O, strongly emit spectral radiation in the 3 - 5 μm band, and though the atmosphere is a good absorber of radiation, it has gaps in the 3-5

μm and 8-12 μm bands. Consequently, the addition of a gas turbine power plant to U. S. Navy warships increases the ships susceptibility to detection, tracking, and targeting by infrared seeking anti-ship missiles. It is possible to redesign the ship so that the mast is far enough away from the hot exhaust plume that damage to electronics does not occur. However, simply moving the mast in relation to plume does not address the increased infrared signature of the ship. Developing a means to reduce the gas turbine exhaust temperature will address both problem of damage to equipment and increase infrared signature.

Northrop Grumman Ship Systems (NGSS) has provided a design of an active cooling system for LHD 8 that consists of two 150 hp axial fans that are each 60 inches in diameter. The system proposed by NGSS requires a significant amount of space, which results in increased weight, complexity and maintenance requirements. The addition of the fan room near and underway replenishment (UNREP) station reduced the amount of space available for cargo handling, and also generated an unacceptable noise hazard. To avoid the noise hazard, reduction in space near the UNREP station, and significant increase in topside weight, it was decided to design a passive cooling system.
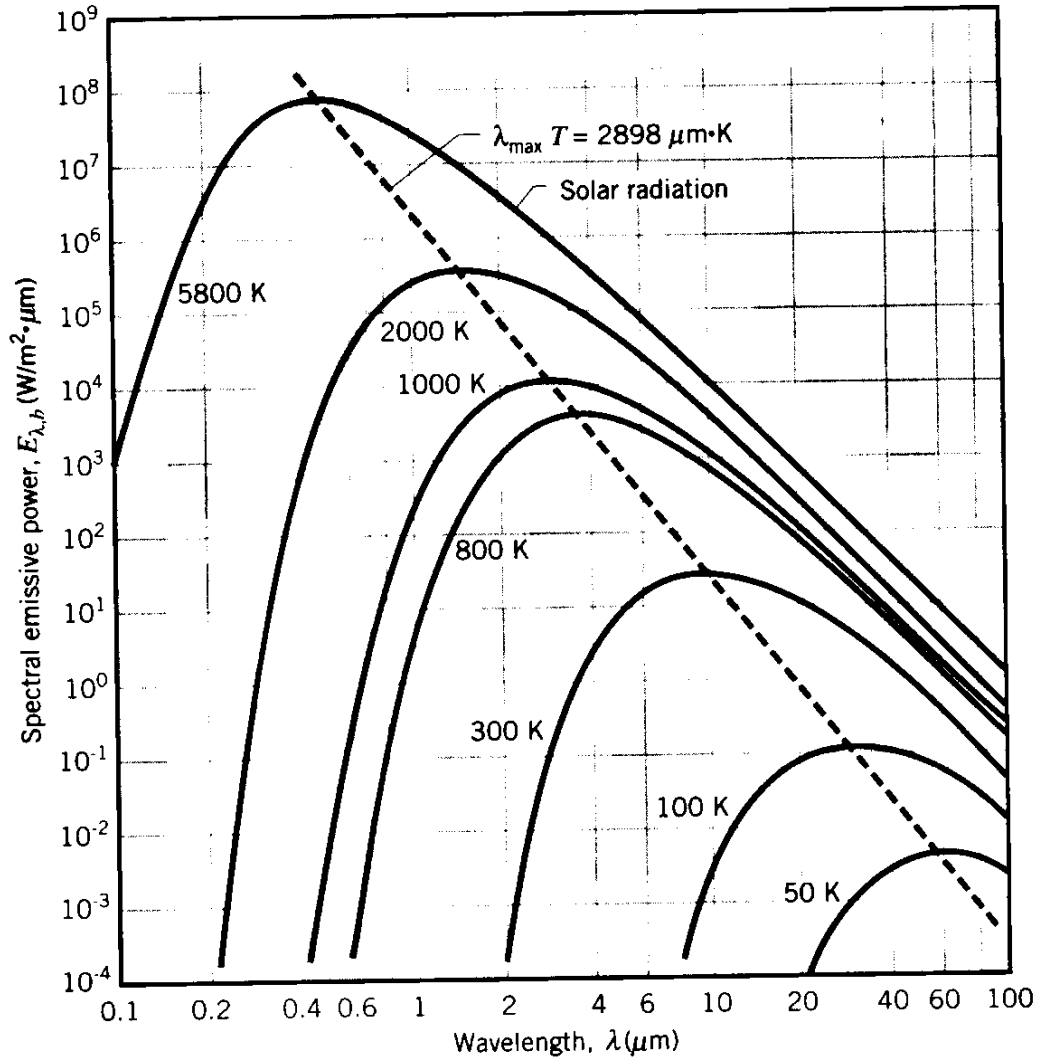
Figure 1 Black Body Emissive Power, from Reference [14].

B.   BACKGROUND

The challenges posed in cooling gas turbine exhaust are not new. Wilsted, Huddleston and Ellis [2] of the National Advisory Committee for Aeronautics (NACA), now known as the National Aeronautics and Space Administration (NASA), researched the effect of temperature on the performance of ejectors for gas turbine exhaust in 1949. In 1953, Hussmann [3] prepared a report for the United States Navy Bureau of Ships, now known as the Naval Sea Systems Command (NAVSEA), that detailed how to design an eductor system for gas turbine powered ships. In 1975, the Navy commissioned USS

SPRUANCE (DD 963), the first large U. S. warship to use gas turbines for propulsion. The gas turbine exhaust cooling system employed on SPRUANCE class destroyers is a single nozzle eductor, similar to the schematic shown in Figure [2], and a Boundary Layer Infrared Signature Suppression (BLISS) cap. The eductor mixes the hot exhaust gases (1) with cool ambient air (2), also known as primary flow and secondary flow respectively. The BLISS cap introduces a thin layer of cool air between the exiting flow and stack surface. The cooler boundary layer reduces the surface temperature of the stack exit and provides some additional cooling of the exhaust gases. The design of the eductor system used on Navy ships has improved over several ship programs. Research at the Naval Postgraduate School, in conjunction with David Taylor Research Center (Annapolis, MD) and NAVSEA began in 1977, Ellin [4], to enhance the mixing of the hot exhaust gases with secondary cooling air by using multiple nozzles vice a single nozzle in the eductor system. The result of this research is the current gas turbine exhaust cooling system used on the TICONDEROGA (CG 47) Class Cruisers and ARLEIGH BURKE (DDG 51) Class Destroyers, Figure [3].
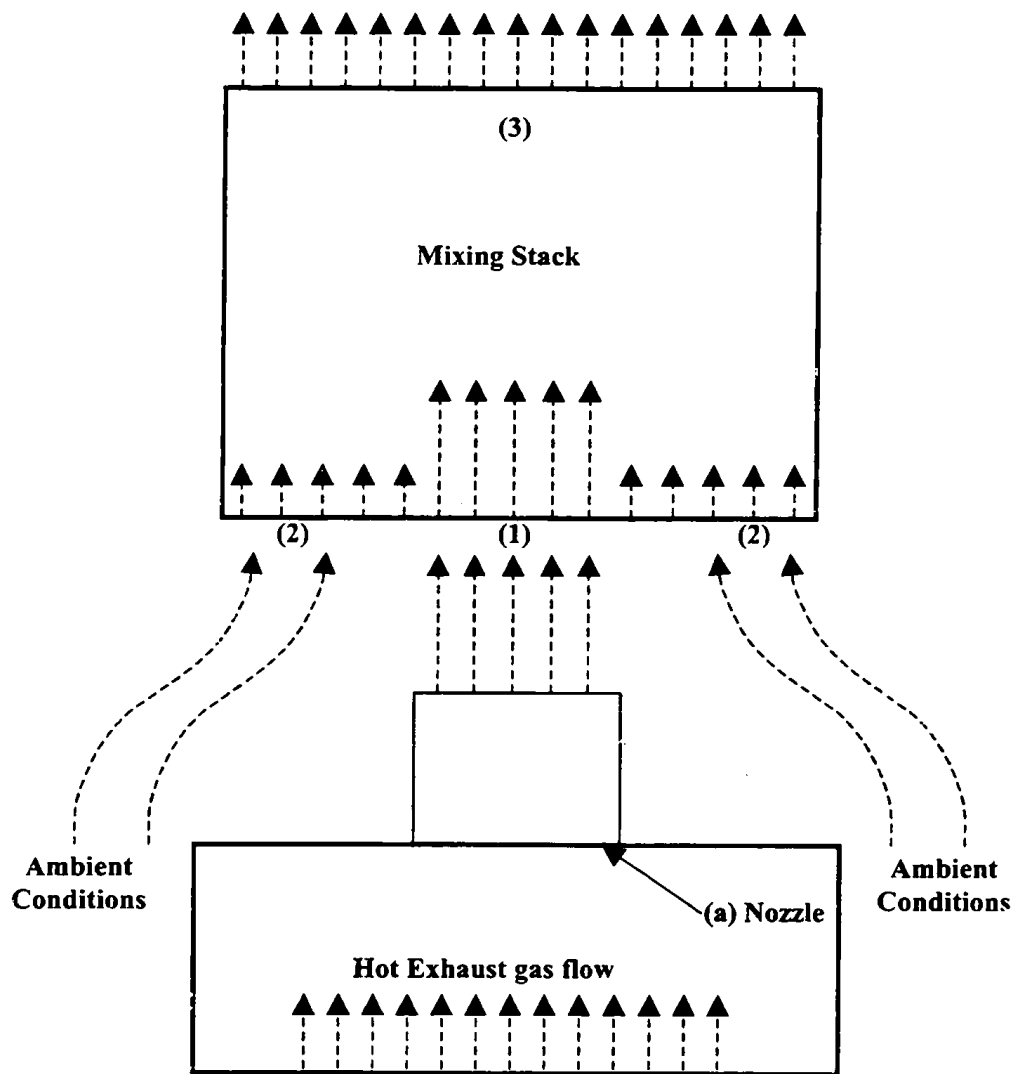
Figure 2 Schematic of a simple eductor, from Reference [6]
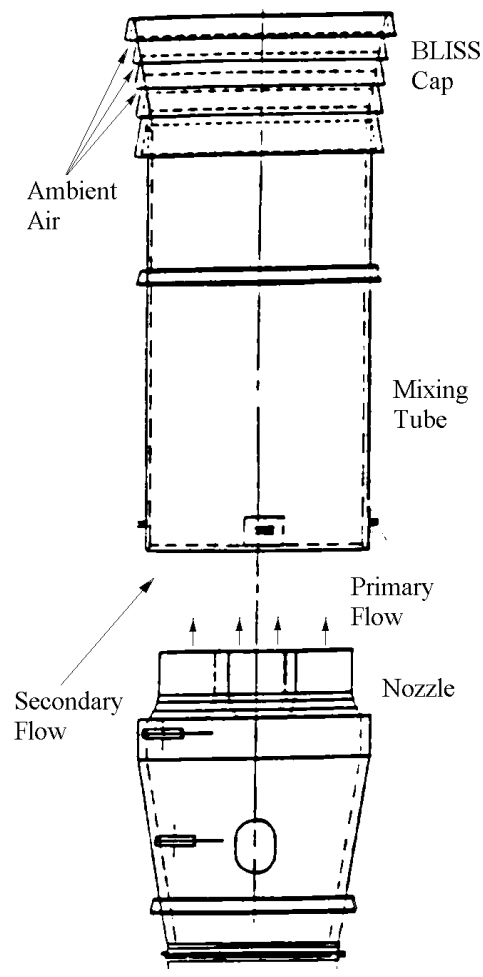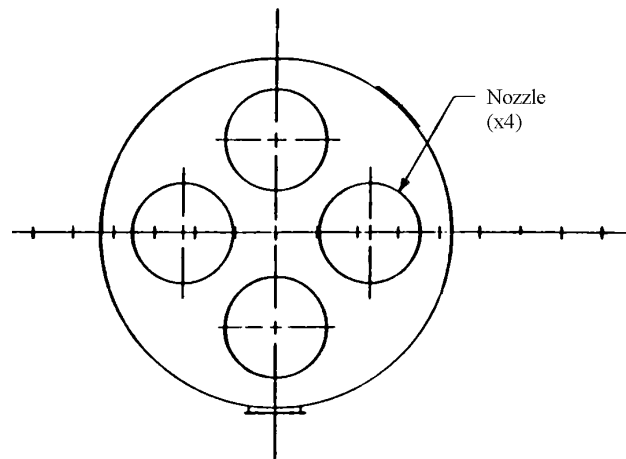
Figure 3 (a) DDG 51 eductor system, (b) Plan view of DDG 51 eductor nozzle, after Reference [9].

Although the eductor systems currently in use on U. S. Navy ships are able to reduce the gas turbine exhaust temperature to a level comparable to that of its steam counter part, the length of the mixing tube is greater than twice the diameter of the mixing tube. In the case of the DDG 51, this results in a mixing tube length of roughly 20 feet. Another successful eductor system developed in Canada is the DRES Ball, Figure [4]. The design allows ambient air to be drawn into the core of the hot primary air, and slightly reduces the amount of topside weight.
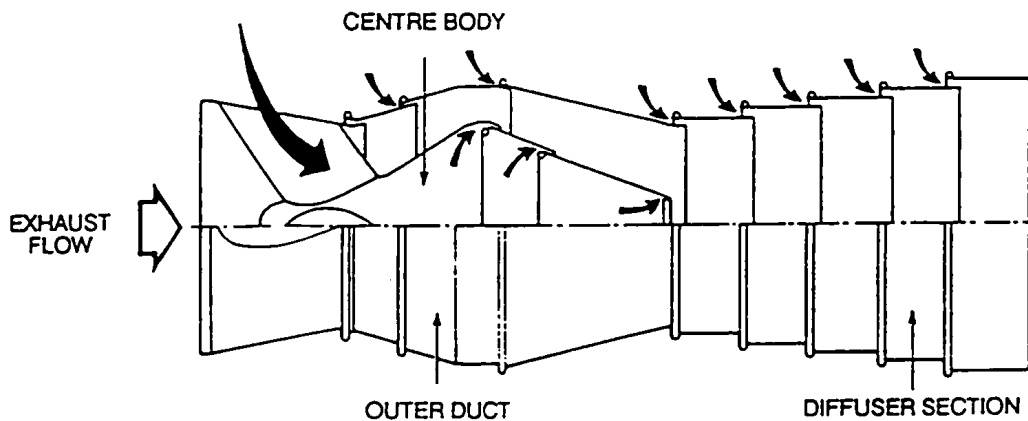
Figure 4 DRES Ball device, from Reference [15].

In an effort to reduce the mixing tube length, and thus, topside structure and weight, a significant amount of research has been conducted in the field of enhanced mixing using lobed nozzles, Figure [5]. In 1987, Presz, Blinn and Morin [5] demonstrated that use of a lobed nozzle could reduce the mixing tube length to diameter ratio (L/D) to nearly unity. Lobed nozzles are used extensively in aircraft applications due to their short mixing length.

Since eductors have proven to reduce the gas turbine exhaust temperature to acceptable levels, it was decided to employ the same technology to the LHA (R). Additionally, a lobed mixer will be used for the nozzle to minimize the amount of topside space and weight added to the ship from using an eductor system.
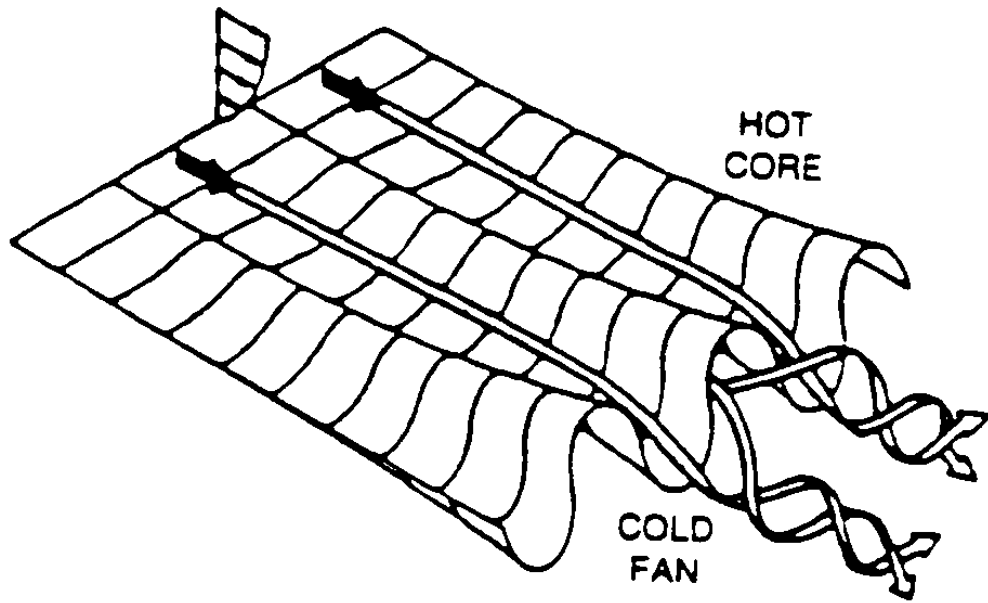
Figure 5 Schematic of a lobed mixer illustrating streamwise vortices, from Reference [5].

C.   OBJECTIVES

The objectives of the research are to:

1. Provide a preliminary design of a passive cooling system for the LHA (R) gas turbine exhaust that meets or exceeds the reduction in temperature that is provided by the DDG 51 exhaust cooling system, and fits within the existing geometry of the LHD 8 uptake space.

2. Estimate the total pressure loss in the proposed system design and compare with the total pressure loss in an uncooled system. The proposed design will include an estimate of the total pressure loss a circular-to-rectangular transition duct.

3. Study the effect of exhaust plume aspect ratio on the radiant intensity for the DDG 51 gas turbine exhaust system. The study will determine if there is a possibility of designing the system with a significant reduction in radiant intensity.

8

D.   ORGANIZATION

Chapter II contains the 1-D model development for the eductor system. The discussion will include assumptions that were made in order to simplify the calculations. This chapter also contains a brief discussion of how the eductor model was validated. The pumping ratio correction factor is explained in this chapter.

Chapter III contains the design studies. The first study varied the mixing tube cross-sectional area, and observed its effect on backpressure. The second study varied the nozzle cross-sectional area, with constant mixing tube exit area, and observed its effect on exit temperature and backpressure. The results from the two studies were used to determine the design point for the eductor system. A comparison of the backpressures and mixing tube exit temperatures for the proposed design and an uncooled system is contained in this chapter.

Chapter IV contains the transition duct design.   The discussion includes development of the geometry and an estimate of the total pressure loss associated with the duct. Validation of the code used to determine the losses is included.

Chapter V contains a study of how changing the circular exit cross-section of the DDG 51 exhaust system to a rectangular cross-section, and then varying the aspect ratio affects the radiant intensity of the exhaust gases.

Chapter VI contains the summary and conclusions.

THIS PAGE INTENTIONALLY LEFT BLANK

II. MODEL DEVELOPMENT AND VALIDATION

A. OVERVIEW AND ASSUMPTIONS

A one-dimensional model of an ideal eductor system was developed to determine the basic geometry required to meet the objectives of this study. Simulating a real, three-dimensional eductor system with a 1-D ideal model required that several assumptions be made including, the flow is uniform, one-dimensional, and uni-axial. Additionally, friction on the mixing tube wall was neglected. Neglecting mixing tube wall friction and assuming uniform flow will overestimate the secondary mass flow rate, and underestimate the mixing tube exit temperature. To account for the errors induced in the ideal model, a correction factor that reduces the predicted entrainment of secondary mass flow will be introduced.

The following assumptions were made in the development of the 1-D ideal eductor model:

1. The flow is uniform, uni-axial and one-dimensional at the nozzle exit, the mixing tube entrance and the mixing tube exit.
2. The flow is incompressible since the maximum velocity in the system, at the nozzle exit, is less than Mach 0.3.
3. The exhaust gases are ideal gases.
4. The properties (density, viscosity, specific heat, etc…) of the exhaust gases are that of air.
5. The density of the exhaust gases in the mixing tube varied axially due to the temperature change from entrance to exit.
6. The walls of the exhaust ducting, including the mixing tube, are adiabatic. However, heat transfer does take place between the flows within the mixing tube
7. The gas turbine provided constant mass flow of exhaust gases ($\dot{m}_a$=189 lbm/s, T_a=910 $^{\circ}$F) at full power.

B.   THE IDEAL ONE-DIMENSIONAL MODEL

The equations used for the model come directly from basic fluid mechanics namely, Continuity, Momentum, Energy and State. Four control volumes were used to analyze the model, the first was around the straight duct section, the second around the transition duct, the third around the nozzle section, and the fourth around the mixing tube. See Figure [7] for clarification. It was assumed the engine provided a constant mass flow of exhaust gasses at a full power setting, and that there are no leaks or sources of air in the ducting from the entrance (station "a") through the nozzle exit (station "3"). Therefore, from continuity

$$\dot{m}_a = \dot{m}_1 = \dot{m}_2 = \dot{m}_3 \tag{1}$$

The following equations were used for the first control volume:

Continuity

$$\dot{m}_a = \dot{m}_1 \tag{2}$$

$$\dot{m}_1 = \rho_1 A_1 V_1 \tag{3}$$

Energy equation

$$\frac{P_a}{\rho_\alpha g} + \frac{V_a^2}{2g} + Z_a = \frac{P_1}{\rho_1 g} + \frac{V_1^2}{2g} + Z_1 + H_{f1} \tag{4}$$

Equations of state

$$P_a = \rho_a R T_a \tag{5}$$

$$P_1 = \rho_1 R T_1 \tag{6}$$

Bernoulli's equation

$$P_{ta} = P_a + \frac{1}{2}\rho_a V_a^2 \tag{7}$$

$$P_{t1} = P_1 + \frac{1}{2}\rho_1 V_1^2 \tag{8}$$

Head loss due to friction

$$H_{f1} = f\frac{Z_1 - Z_a}{D_{ha}}\frac{V_a^2}{2g} \tag{9}$$

12

Where the Darcy friction factor (f) was assumed to be 0.01 for new stainless steel based on the duct hydraulic diameter, and Z_i (i=a, 1…) is the height of the station cross-section.

In similar fashion, the following equations were used for the second control volume:

Continuity

$$\dot{m}_1 = \dot{m}_2 \tag{10}$$

$$\dot{m}_2 = \rho_2 A_2 V_2 \tag{11}$$

Energy equation

$$\frac{P_1}{\rho_1 g} + \frac{V_1^2}{2g} + Z_1 = \frac{P_2}{\rho_2 g} + \frac{V_2^2}{2g} + Z_2 + H_{f2} \tag{12}$$

Equation of state

$$P_2 = \rho_2 R T_2 \tag{13}$$

Transition duct losses

$$H_{f2} = \zeta_t \frac{V_2^2}{2g} \tag{14}$$

Where ζ_t is the total pressure loss coefficient for the transition duct. A detailed explanation of how ζ_t was determined is contained in chapter IV.

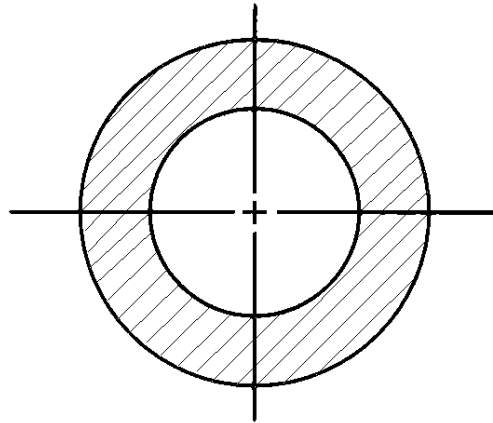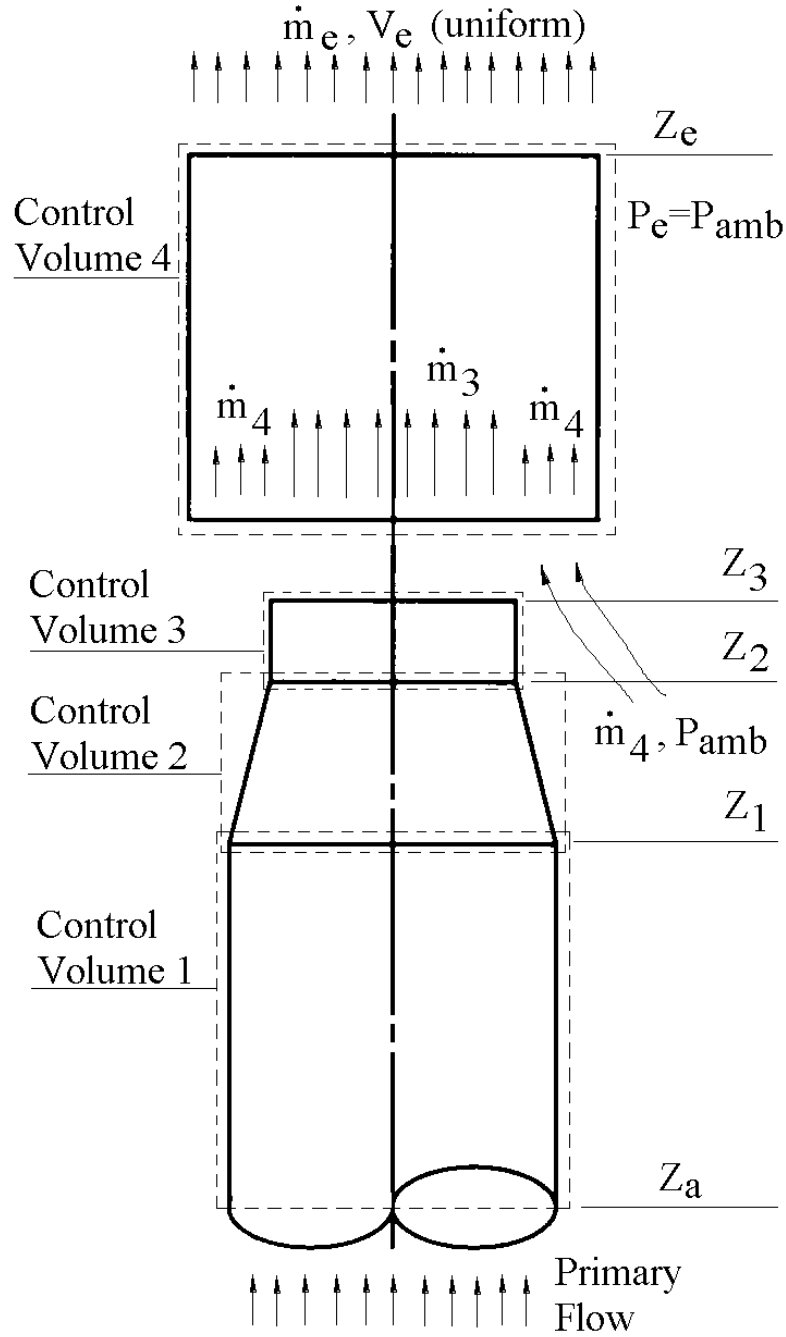Figure 6 Plan view of mixing tube, Area A$_4$ is shaded.

13

Figure 7 Station labeling of eductor system.

The nozzle section again used the same equations as the transition duct with the exception of the total pressure loss coefficient. The losses for the nozzle section were assumed to be $\zeta_n = 0.1$ since the actual total pressure loss is a function of the lobed nozzle geometry as determined in reference [5].

The amount of secondary air required was determined using the following equations:

Equation of state

$$P_4 = \rho_4 R T_4 \tag{15}$$

$$\dot{m}_4 = \rho_4 A_4 V_4 \tag{16}$$

Bernoulli's equation for secondary air

$$P_{t4} = P_4 + \frac{1}{2} \rho_4 V_4^2 \tag{17}$$

It was assumed that static pressures of the primary flow at the nozzle exit and the secondary flow at the mixing tube entrance were equal.

$$P_4 = P_3 \tag{18}$$

Finally, the equations used for the fourth control volume are as follows:

Continuity

$$\dot{m}_a + \dot{m}_4 = \dot{m}_e \tag{19}$$

$$\dot{m}_e = \rho_e A_e V_e \tag{20}$$

$$A_e = A_3 + A_4 \tag{21}$$

For clarification, A_4 is shown as the shaded area in Figure [6]. The Momentum equation is given by

$$\dot{m}_e V_e - \dot{m}_3 V_3 - \dot{m}_4 V_4 = P_3 A_3 + P_4 A_4 - P_e A_e \tag{22}$$

Energy equation

$$\dot{m}_3 (\frac{\gamma}{\gamma-1} R T_3 + \frac{1}{2} V_3^2) + \dot{m}_4 (\frac{\gamma}{\gamma-1} R T_4 + \frac{1}{2} V_4^2) = \dot{m}_e (\frac{\gamma}{\gamma-1} R T_e + \frac{1}{2} V_e^2) \tag{23}$$

Equation of state

$$P_e = \rho_e R T_e \tag{24}$$

All the equations previously mentioned in this section were written into an Engineering Equation Solver (EES) code and solved simultaneously. The EES software solves the equations by iteration to a specified tolerance using the known values as defined by the user, such as ambient conditions, gas turbine exhaust mass flow rate and

temperature, and user defined guesses for the unknown variables. The EES code that was written for this study is contained in Appendix A.

C.   MASS FLOW CORRECTIONS AND VALIDATION

As was stated in the assumptions for this study, the wall friction in the mixing tube was neglected for the ideal calculations. This assumption results in an overestimate of the secondary mass flow rate and an underestimate of the mixing tube exit temperature. In order to correct the model and obtain realistic secondary mass flow rate and mixing tube exit temperature, a correction factor (cf) was applied to the ideal secondary air mass flow rate in the following manner

$$W_{corr} = (cf)W \tag{25}$$

Where the pumping ratio W is defined as

$$W = \frac{\dot{m}_{secondary}}{\dot{m}_{primary}} \tag{26}$$

The equations for the fourth control volume were then recalculated using the corrected pumping ratio to determine the real mixing tube exit temperature.

The correction factor was obtained from a combination of empirical data found in Keenan [8] and Otis [6]. The data from Keenan, shown in Figure [8], are the ratio of measured mass flow to calculated mass flow versus the ratio of nozzle total pressure to ambient pressure.
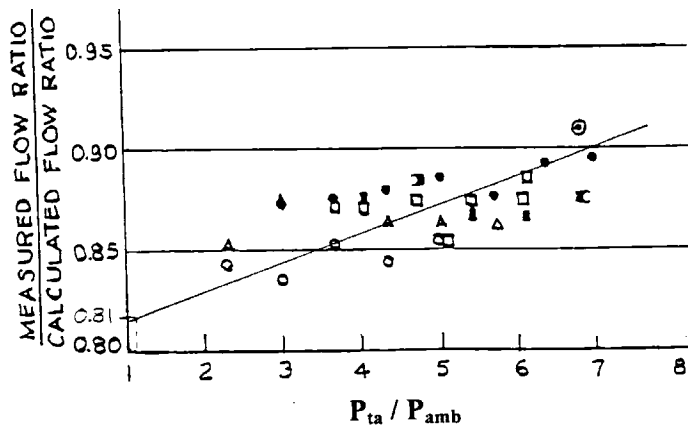

Figure 8 Ratio of mass flow ratios versus pressure ratio, from Reference [6].

16

A best-fit curve was applied to the data to determine a correction factor. For purposes of model validation, full power for the LM2500 was used, where $\dot{m}$ =153 lbm/s, plus 20 lbm/s module cooling air, and T_a=807 ^{o}F, taken from Reference [7]. Since the pressure ratio for the DDG 51 eductor nozzle is only slightly greater than unity, the correction factor, from the graph is 0.81. Based on his model validation, Otis [6] determined that the correction factor should be 0.79 in order to produce the temperature found at the exit plane of the DDG 51 mixing tube. Since the ideal model for this study indicated that the pressure ratio was also only slightly higher than unity, it was decided to use a correction factor of 0.8. To validate the model used in this study, the data used by Otis [6] for the DDG 51 along with the appropriate nozzle loss coefficient was used. The exit temperature calculated by the model differed by less than 1% compared to the value found in Reference [9] for DDG 51.

The backpressure that the eductor system would develop was calculated, since increased backpressure decreases engine performance. Engine backpressure, as defined in Reference [9] is the difference between the static pressure measured at the engine module exit and ambient pressure. Since the exhaust configuration for LHA (R) from the 02 level to the engine module is not known, backpressure is defined as the difference between the predicted static pressure at the 02 level and the ambient pressure. The backpressure limit for the LM2500 with an eductor system, from Reference [7] is 12 inches H_2O. For the purpose of this study, the same backpressure limit was assumed for the LM2500+. Again, using information taken from DDG 51, the backpressure calculated by the model was within 18% of the measured value from Reference [9]. The backpressure calculated by Otis [6] for the DDG 51 was within 17% of the value listed in Reference [9]. Based on the small error between the calculated value and the actual exit temperature, and the agreement in calculated backpressures, it was determined that the code was accurate in predicting mixing tube exit temperature and secondary air mass flow.

THIS PAGE INTENTIONALLY LEFT BLANK

III.   PRELIMINARY DESIGN STUDY

A.   TRADE STUDY USING THE 1-D CORRECTED MODEL

The corrected and validated eductor model discussed in the previous chapter was used as the primary design tool for this study. The first step in performing the study was to change the values used in the model to those of the LM2500+. The values used for exhaust mass flow ($\dot{m}$ = 189 lbm/s plus 20 lbm/s module cooling air) and turbine exit temperature (T_a= 910 $^{\circ}$F) were determined by the Naval Surface Warfare Center, Carderock Division, these values differ slightly from those quoted by General Electric Aircraft Engines Division [16], where $\dot{m}$ = 189 lbm/s and Ta = 965 $^{\circ}$F.

The next step was to determine the available volume of the existing LHD 8 uptake space. This established the maximum size that would be allowed for the mixing tube since the mixing tube has the largest cross-section of the exhaust ducting. Since the design for the LHA (R) superstructure and uptake space was not available for this study, it was assumed that the uptake space for the LHA (R) was identical to that of the LHD 8. With the knowledge of what the maximum cross-sectional area could be for the mixing tube, several mixing tube cross-sectional areas were chosen and the nozzle exit area varied for each case. At this point in the design process, the transition duct exit area was neglected in order to establish the nozzle exit area. The analysis shown in Figure [9] determined that the mixing tube area to nozzle area (A_e/A_3) was 3.1 for each case, where the goal was to have a pumping ratio of unity. It is also evident in Figure [10] that as the mixing tube area decreases the backpressure increases. Noting the trend of backpressure as a function of mixing tube area, it was decided to use the largest possible mixing tube that would fit into the uptake space.
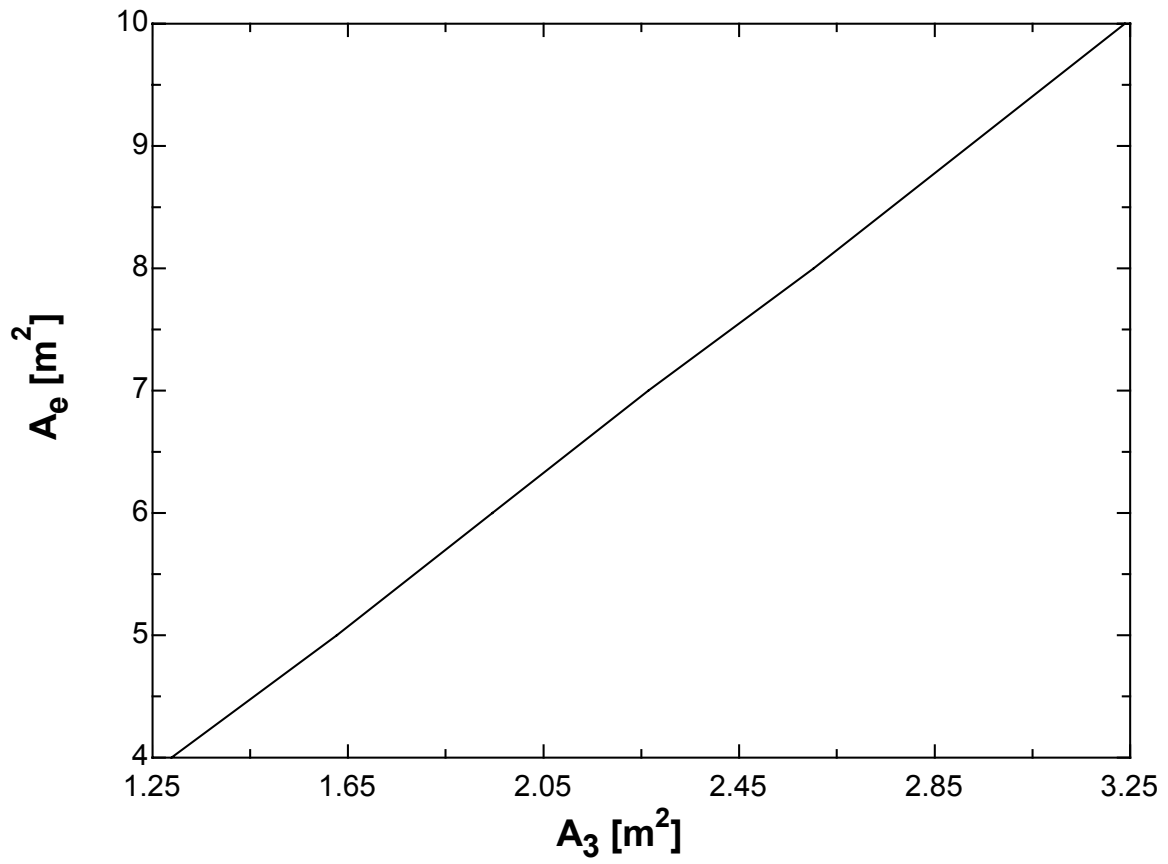
Figure 9 Mixing tube exit area versus Nozzle exit area for a pumping ratio of unity.
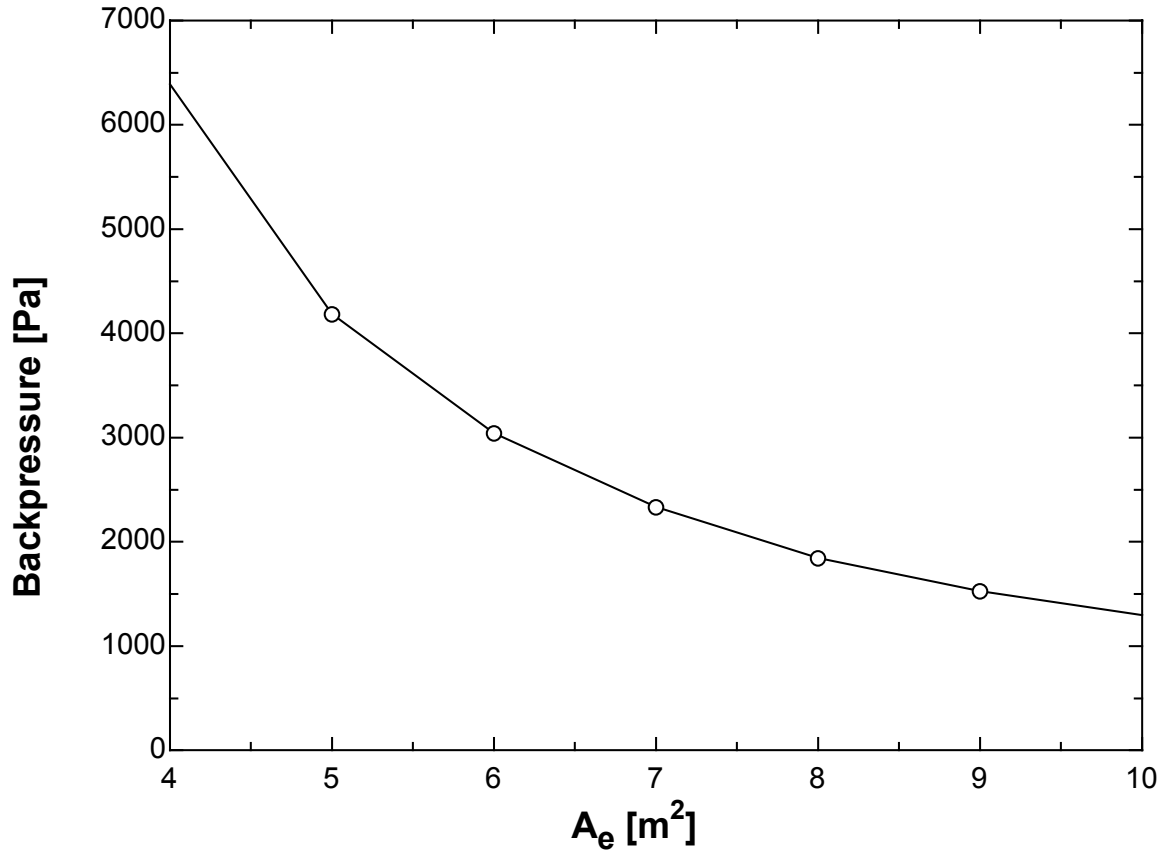
Figure 10 Backpressure versus mixing tube exit area for $A_e/A_3=3.1$ and W=1.

Once the mixing tube area was established, the next step in the design process was to determine the nozzle exit area. Finding the nozzle exit area was performed in the same manner, as was the mixing tube area. By varying the nozzle exit area and noting where that area achieved a pumping ratio of unity, the correct nozzle area could be determined for the given primary flow conditions. Figure [11] is a graphical representation of both backpressure and exit temperature as a function of nozzle exit area.
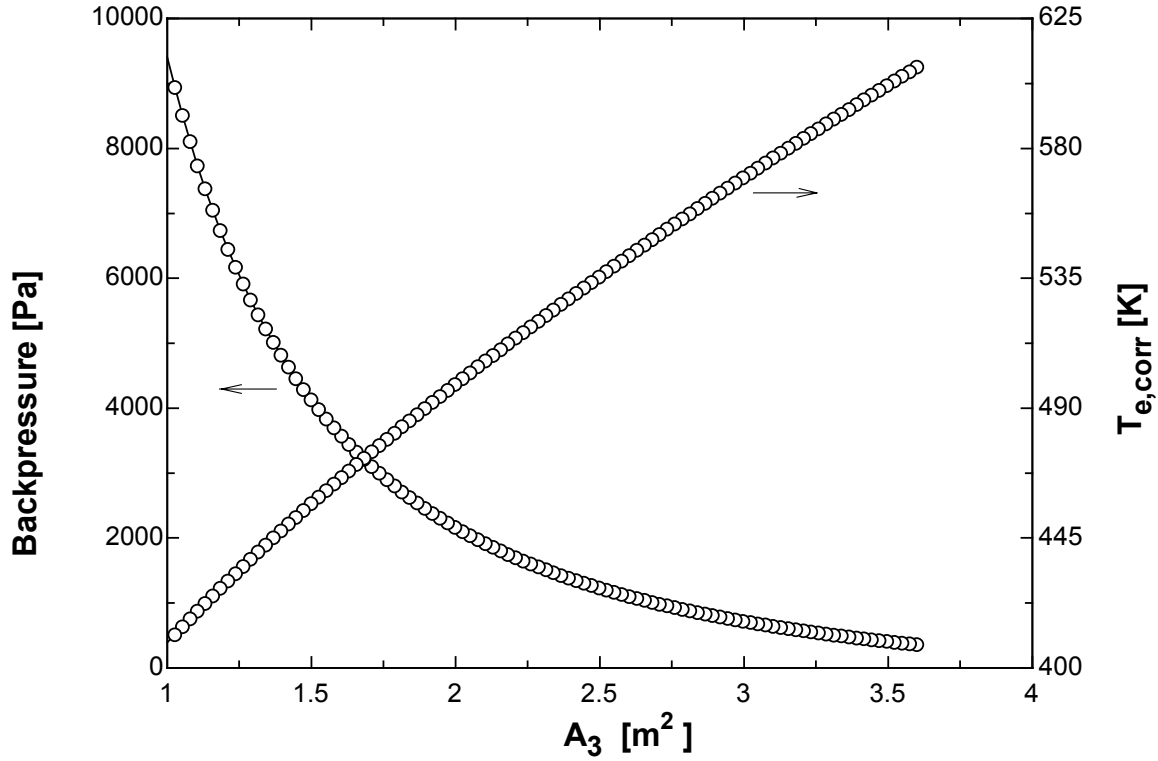
Figure 11 Backpressure and exit temperature versus nozzle exit area for a constant mixing tube exit area.

Now that the nozzle exit area was known, the exit area of the transition duct could be fixed and the final design complete. The transition duct exit area was set to be larger than the nozzle exit area so that the cross-section constantly decreased through the nozzle.

The selected nozzle area and mixing tube area resulted in an exit temperature that was 12% lower than that achieved by the DDG 51 eductor system, at the cost of a 6 in H_2O increase in backpressure, as compared to a straight exhaust duct without cooling.

B.   EDUCTOR DESIGN

Now that the general cross-sectional areas have been selected, it was necessary to make them fit within the available space in the existing uptake space.   This was accomplished by squeezing the two diesel generator exhausts into one-fifth of the available area of the uptake space, and flattening out the gas turbine exhaust with an oval-

to-rectangular transition duct. In order to accomplish the rerouting of the diesel exhaust, a similar study was conducted using the same 1-D model, substituting the diesel exhaust parameters. Results of the diesel exhaust study are contained in Appendix B. The resultant design proposed for the LHA (R) uptakes are shown in Figures [12] and [13].
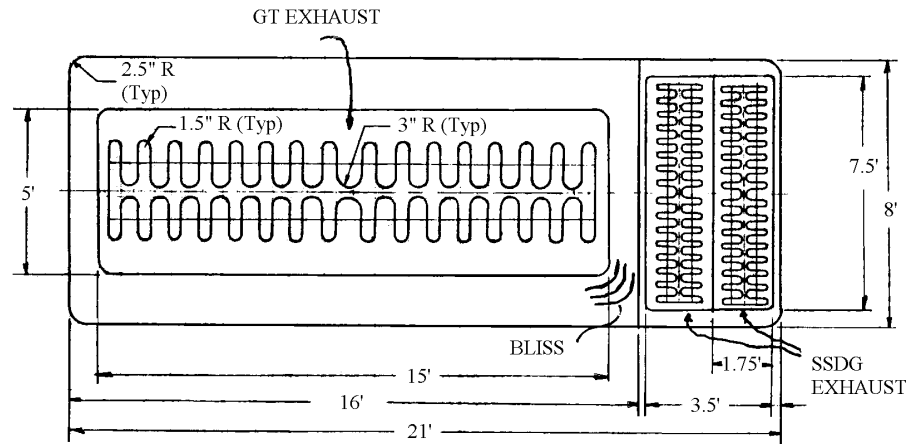
Figure 12 Plan view of proposed LHA (R) exhaust system.

Top 61.75'

GT MIXING TUBE

SSDG MIXING TUBE

08 55.25'

SSDG NOZZLES

07 46.75'

GT NOZZLE

06 38.25'

05 29.75'

AMBIENT AIR

04 21.25'

03 9.75'

02 0'

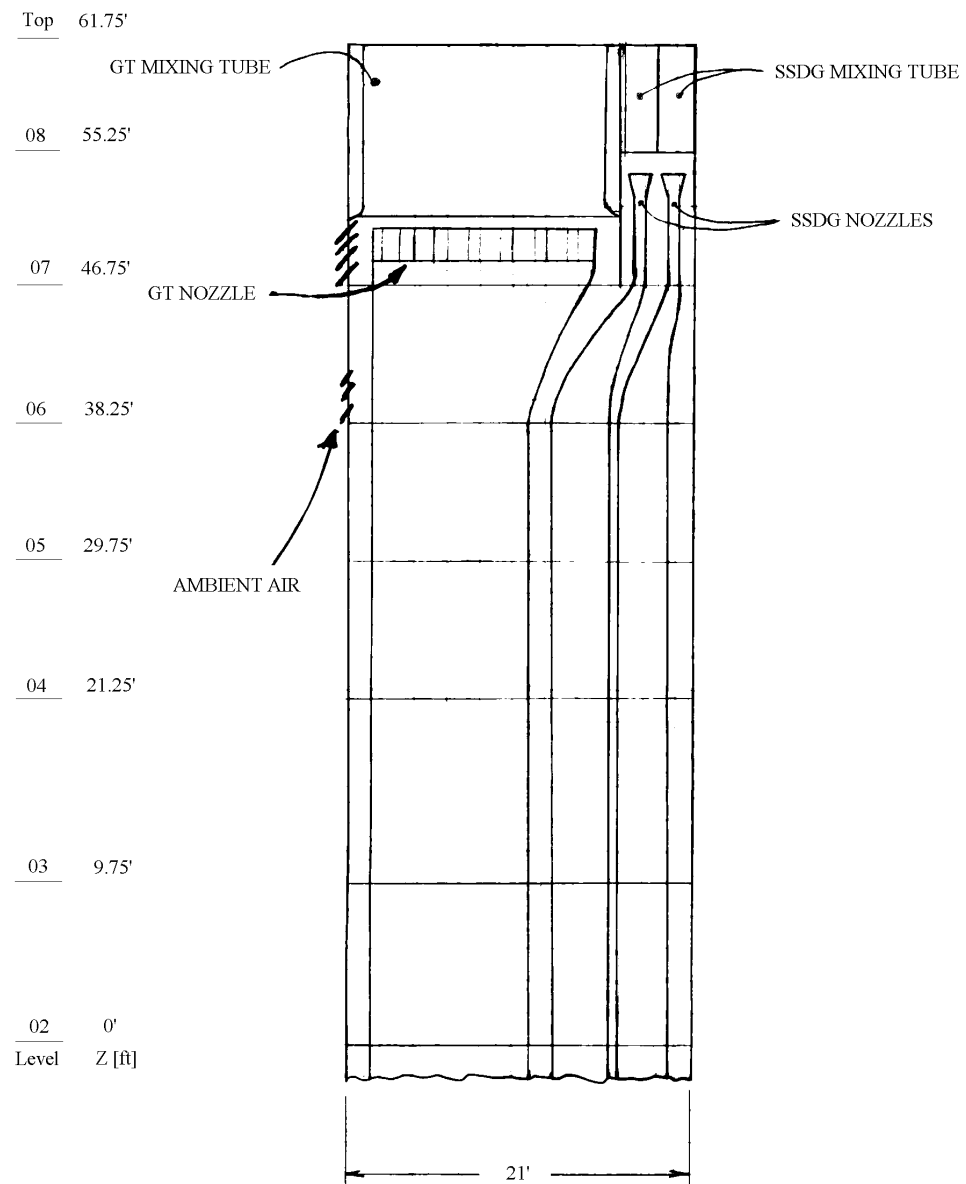Level Z [ft]

21'

Figure 13 Elevation of proposed LHA (R) exhaust system.

The proposed design begins at the 02 level. The gas turbine exhaust consists of the existing flat oval duct, an oval-to-rectangular transition duct, a lobed nozzle, and mixing tube. The diesel exhaust consists of the existing flat oval duct that transitions through an "S" duct into a flat rectangle with a lobed nozzle and mixing tube. The secondary air intakes for the gas turbine and diesel exhausts are to be separated so that the diesel eductor is not starved by the gas turbine eductor.

C.   BACK PRESSURE COMPARISON

The following is a comparison of backpressure between the proposed LHA (R) eductor system and an uncooled LHA (R) gas turbine exhaust. Figure [14] shows the change in static and total pressure for each section of ducting, measured in "H_2O. As previously mentioned in Chapter II, backpressure is defined as the difference between the predicted static pressure at the 02 level and the ambient pressure. The addition of the eductor components adds approximately 6 "H_2O backpressure to the system as proposed. The backpressure in the eductor system could be lowered at the cost of increased exit temperature, see Figure [11]. Conversely, the exit temperature could be reduced further if increased backpressure is allowed.

D.   THE LOBED NOZZLE

A lobed nozzle was selected for the eductor system because of its enhanced mixing characteristics. The lobed nozzle takes advantage of differences in velocity and density between the primary and secondary flows. As the higher velocity, lower density primary flow meets the slower, higher density secondary flow, a streamwise vortex is generated, as shown Figure [5]. The vortices result in more rapid mixing of the two flows. This vortex driven mixing allows for a reduction in the length of the mixing tube. Reduction of the larger mixing tube will result in space and weight savings over traditional eductor systems.
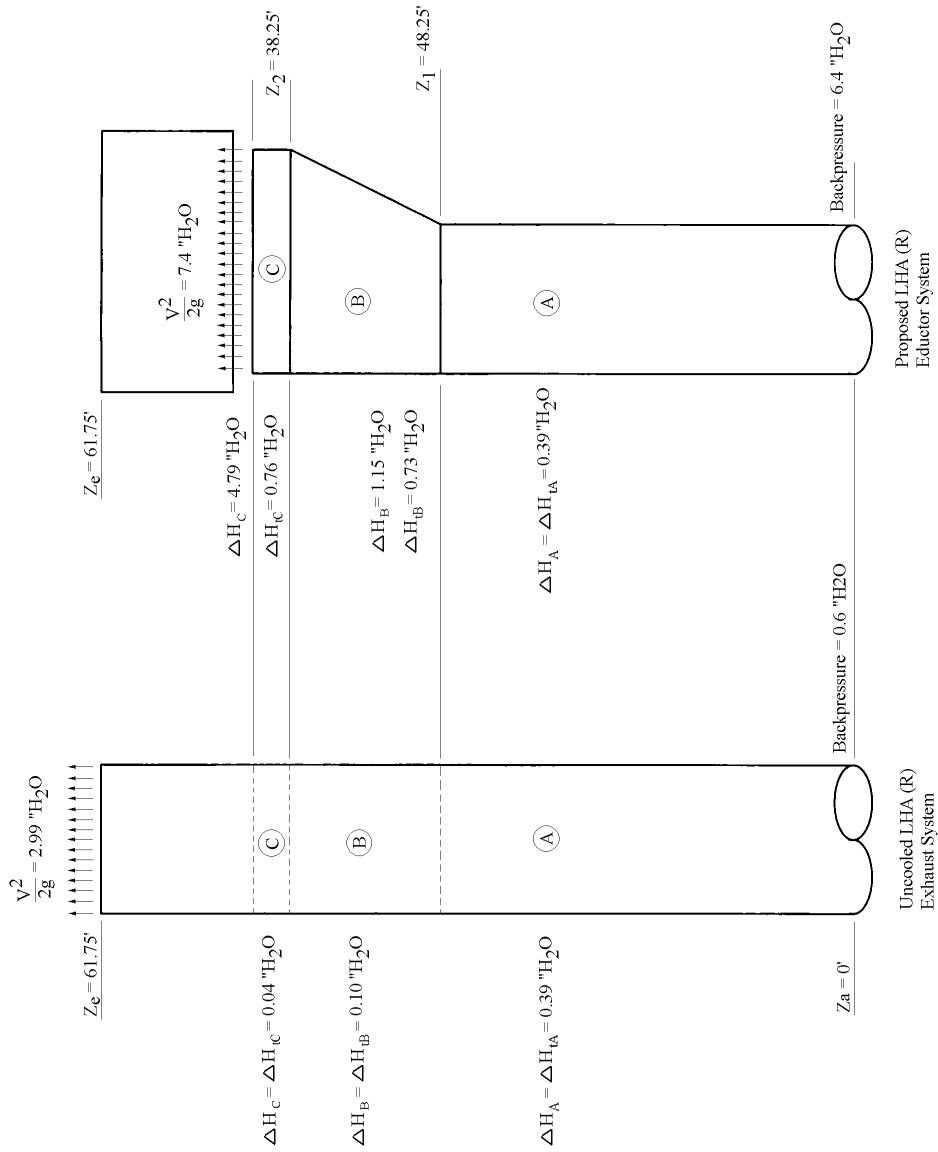
Figure 14 Comparison of backpressures for cooled and uncooled LHA (R) exhaust.

IV. TRANSITION DUCT DESIGN

A. CREATING THE TRANSITION

The transition required going from a flat oval cross-section to a flat rectangular cross-section with an aspect ratio (L/W) of approximately 6:1, with the "x" axis shifting to one side, and an inlet to outlet area ratio (A_1/A_2) of unity. Though many references exist for circular-to-rectangular transitions (e.g. Reference [10]), they do not address transitions of the complexity required for the duct used in this study. Complex transition geometries are employed on stealth aircraft. However, the data for those geometries are highly classified. Therefore, it was determined to use the AR630 transition duct, Figure [15] found in Patrick and McCormick [11], as a starting point. The AR630 duct cross-sectional areas are determined mathematically by use of a super ellipse. The equation for a super ellipse is

$$\left(\frac{y}{a}\right)^m + \left(\frac{z}{b}\right)^n = 1 \tag{27}$$

Figure 15 AR630 transition duct, from Reference [11].

27

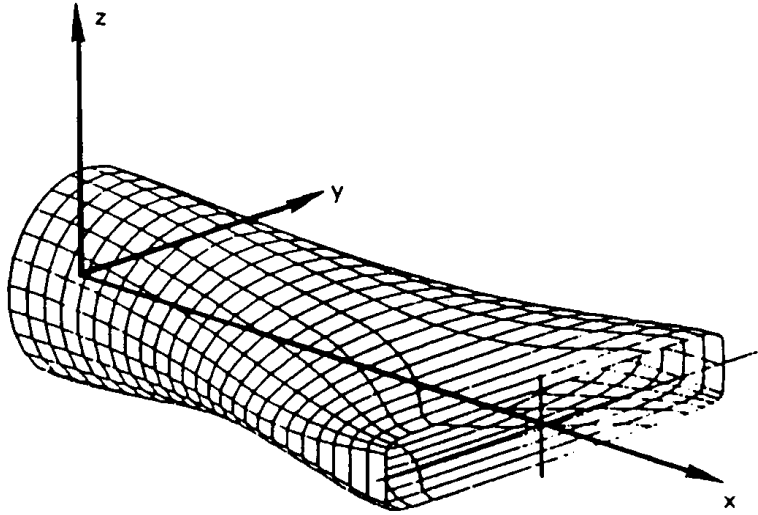The challenge would be to apply a super ellipse equation to begin as a flat oval and transition to a flat rectangle with a longitudinal axis that shifts approximately 2.5 feet. The modified super ellipse equation used in this study is

$$\left(\frac{y+c}{a}\right)^{my} + \left(\frac{z}{b}\right)^{nz} = 1 \tag{28}$$

where the coefficients my, nz, a, b and c are all functions of axial distance. The coefficients versus axial distance, along with the code that was used to calculate the transition geometry are listed in Appendix C. Figure [16] illustrates the geometry produced by equation (28) for this study.
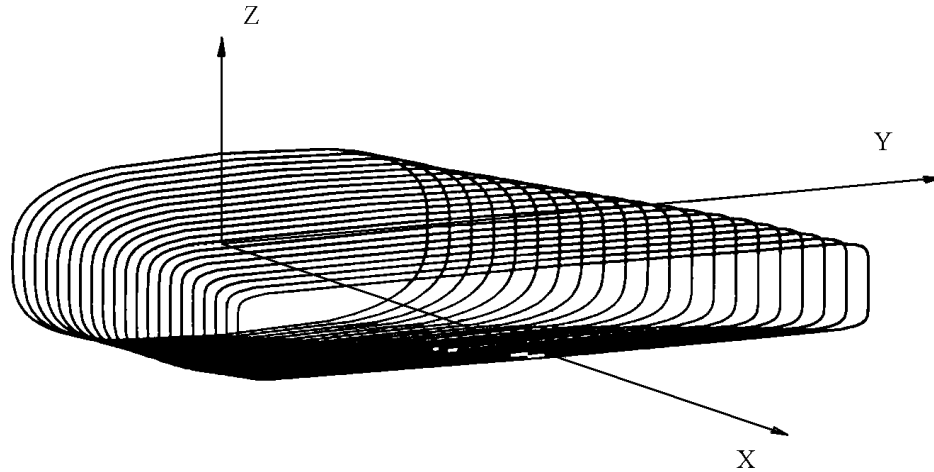
Figure 16 Transition duct for proposed LHA (R) exhaust system.

B. TOTAL PRESSURE LOSS IN THE TRANSITION

To produce a more accurate estimate of the performance for the eductor design, the total pressure loss through the transition duct must be known. Since the losses for the duct designed in the previous section are not known, it was decided to use the losses found in the AR630 duct. The geometries are similar, in that the aspect ratios and the area ratios for both ducts are nearly 6:1 and 1:1 respectively. Although Patrick and McCormick [11] provided a detailed report on the AR630 duct, they did not produce a

total pressure loss coefficient for the entire duct. Rather, the report showed dimensionless velocity and pressure profiles for both inlet and outlet cross-sections. The report also included tabular data that was used to generate the outlet profiles. The total pressure loss coefficient in the AR630 duct was determined by the equation

$$\zeta_t = \frac{P_{t1} - P_{tref}}{Q_{ref}} \tag{29}$$

and

$$Q_{ref} = \frac{1}{2}\rho V_{ref}^2 \tag{30}$$

where V_{ref}=100 ft/s and P_{tref}=14.7 psia.

The total pressure at the inlet of the AR630 duct was determined by generating similar dimensionless velocity and total pressure profiles in MATLAB. In order to obtain the slug profiles found in Figures [17] and [18], a super ellipse of the form found in equation (27), (where a=1, b=1, m=10 and n=10) was used. Figures [18] and [19] are the inlet velocity and total pressure profiles, for the AR630 duct, generated by the code.
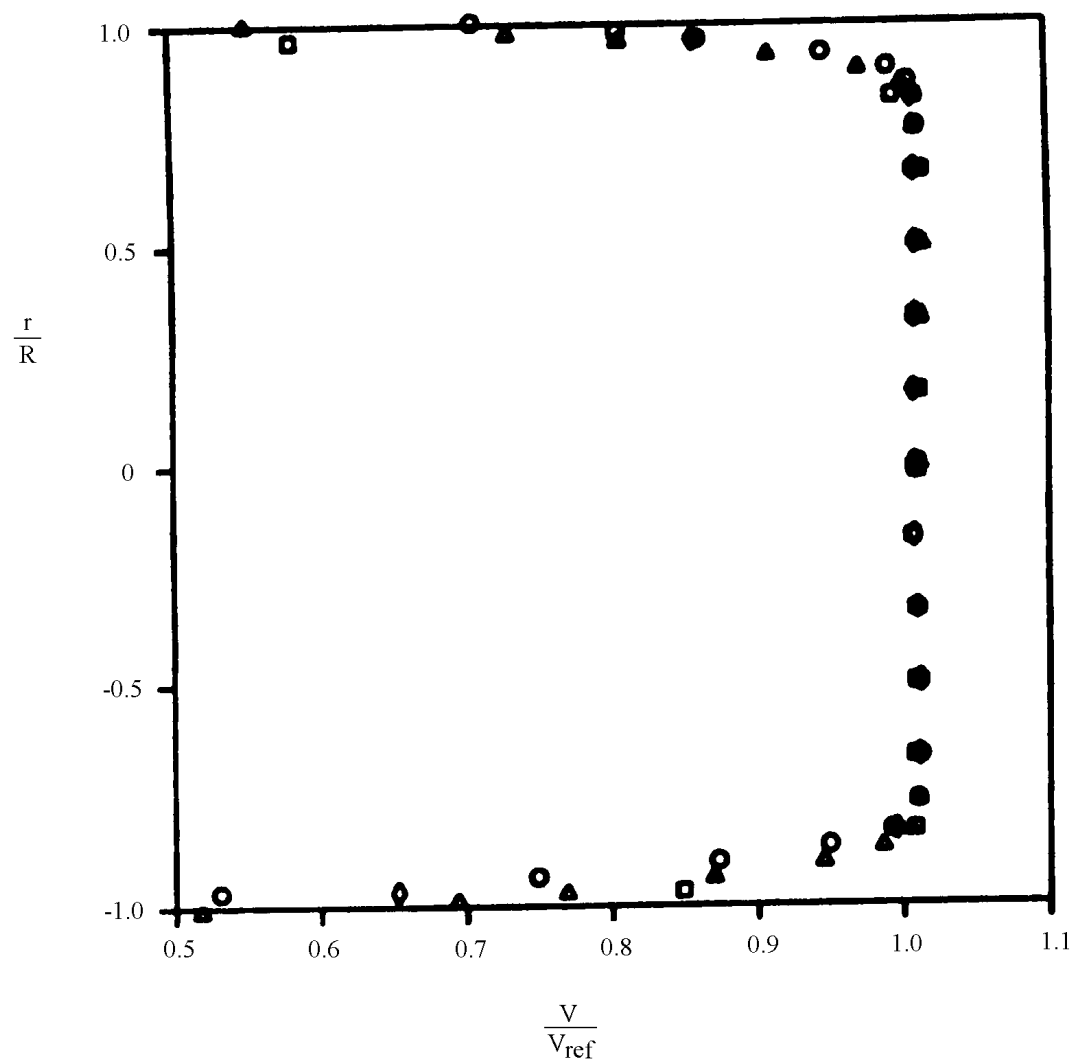
Figure 17 AR630 inlet velocity profile, after Reference [11].
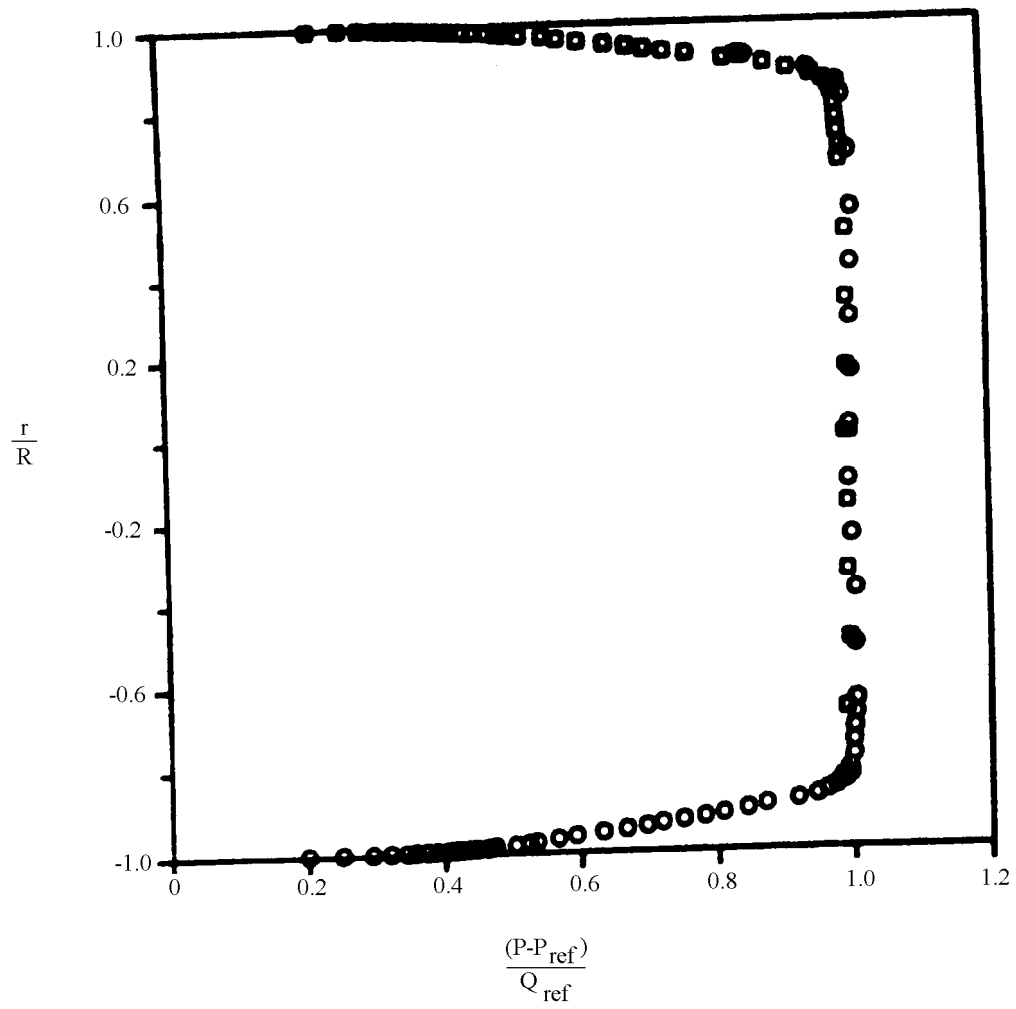
Figure 18 AR630 inlet total pressure profile, after Reference [11].
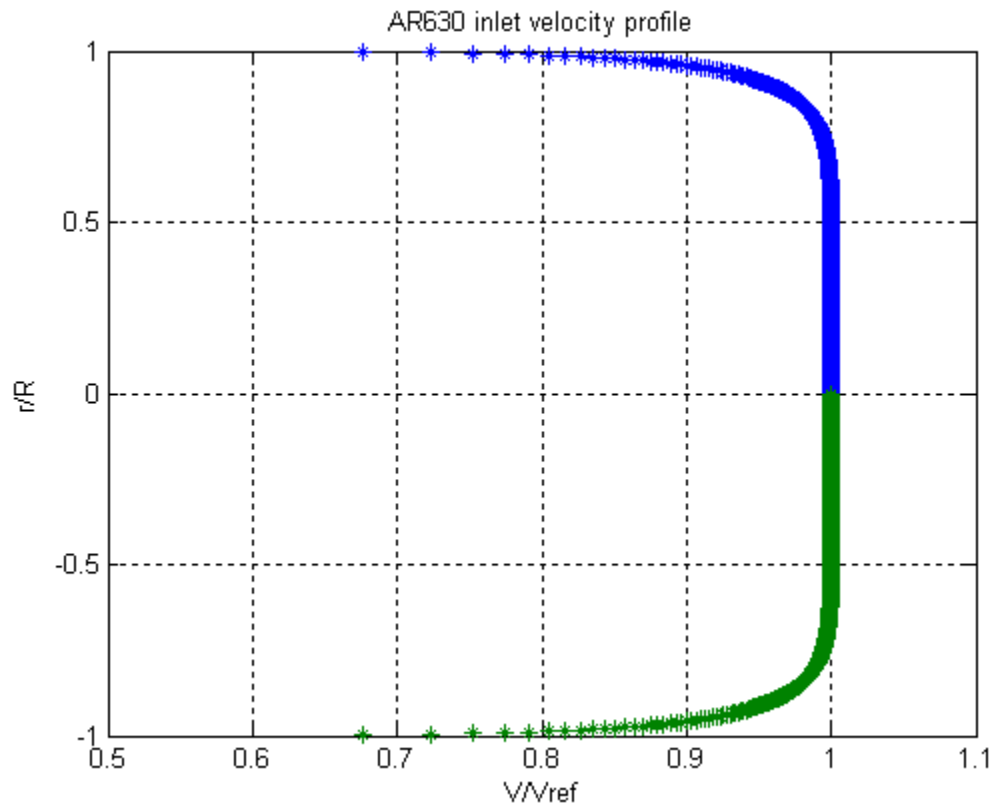
Figure 19 AR630 inlet velocity profile generated in MATLAB.
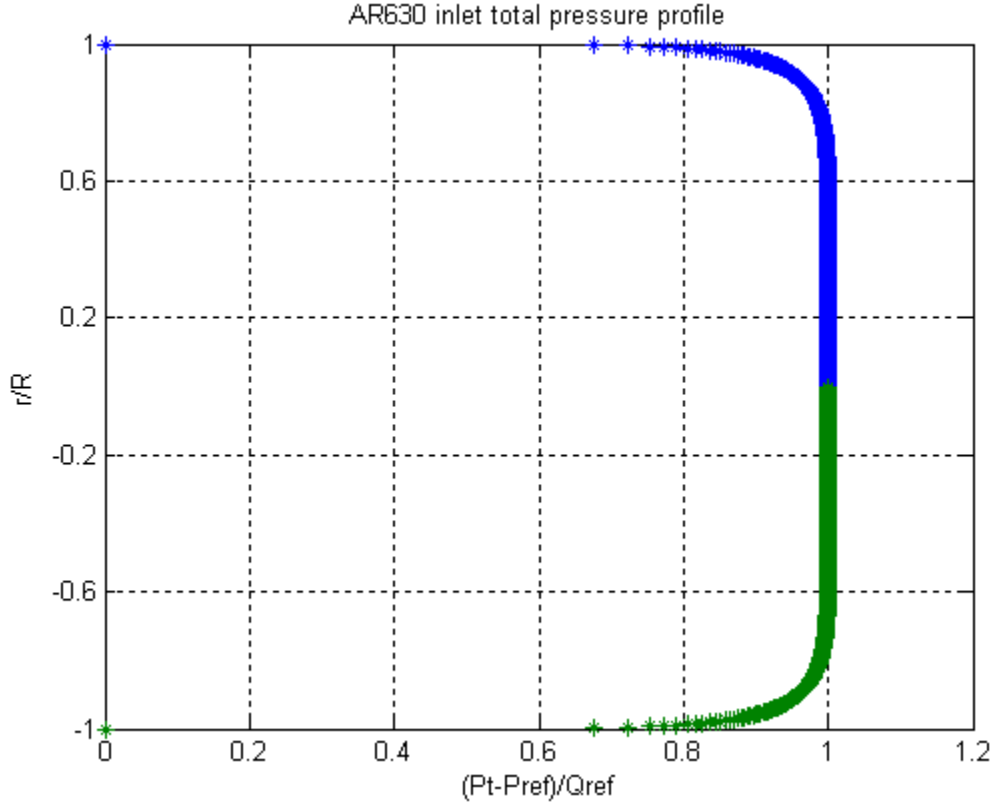
Figure 20 AR630 inlet total pressure profile generated in MATLAB.

Once, the profiles were calculated, the pressure was integrated over the cross-section using the equation

$$P_t = \frac{\rho \iint V(x,y)P_t(x,y)dA}{\rho \iint V(x,y)dA} \tag{31}$$

The double integral was calculated using MATLAB. The results of the calculation yielded the total pressure at the duct inlet.

Similarly, the tabular data provided for the outlet to the AR630 duct was integrated over the exit cross-section yielding the exit total pressure. The inlet and outlet total pressures were then substituted into Equation (29) to determine the total pressure loss coefficient (ζ_t) for the duct, which was estimated as, $\zeta_t = 0.2$. The code used to calculate the loss coefficient is provided in Appendix D.

C.   VALIDATION OF THE LOSS COEFFICIENT

To ensure that integrating the inlet and outlet pressure of the duct in the manner described in the previous section produced the correct loss coefficient, a simple model was developed to test the code.   The model was a simple, gradually converging concentric nozzle with a flow area ratio of 2:1. From White [12], for such a nozzle, the total pressure at the nozzle exit is 95% that of the total pressure at the inlet.   Using the super ellipse code to develop the dimensionless velocity and pressure profiles for the inlet and outlet of the nozzle and integrating over each cross-section, then substituting the total pressures into equation (29) resulted in a loss coefficient of 0.049.   The calculated and known values for the loss coefficient, for the model case, differ by 3%.   Based on the low error, the code used to determine the loss coefficient for the AR630 duct produced accurate results.

V. PLUME RADIATION STUDY

A. OVERVIEW AND ASSUMPTIONS

The purpose of this study is to determine how much the radiant intensity of a gas turbine exhaust plume can be reduced if the mixing tube exit geometry is a high aspect ratio slot vice the current circular cross-section. The study will focus on CO_2 and H_2O in the 3-5 μm band, since both CO_2 and H_2O emit strongly in this band for the temperature range of the exhaust gases. Several assumptions were made in order to estimate the plume's radiant intensity, including that the plume is homogeneous and isothermal, and does not contain soot. Additionally, it was assumed that the atmosphere was a non-participating medium.

The study used empirical data taken from Reference [9] for DDG 51 and the LM2500 gas turbine engine at full power from Reference [7]. The data from Reference [9] provided a real plume temperature, while Reference [7] provided the information necessary to determine the partial pressures of CO_2 and H_2O in the DDG 51 exhaust plume. Since the LM2500 uses either JP-5 or Diesel Fuel Marine, both of which consist of several different types of fuels and have no specific chemical designation, it was assumed that the chemical composition of the fuel was $C_{10}H_{19.185}$. The composition resulted in partial pressures of 5% for both CO2 and H20 given a fuel-to-air ratio (*f*) of 0.0224.

The following assumptions were made in order to estimate the intensity of a gas turbine exhaust plume:

1. The plume was isothermal and homogeneous.
2. The plume consisted of the by-products of complete combustion only.
3. The atmosphere was a non-participating medium.
4. The chemical composition of the fuel used in U. S. Navy marine gas turbines was $C_{10}H_{19.185}$.

B.   THE EXPONENTIAL WIDE BAND MODEL

According to Modest [13], the Exponential Wide Band Model "is by far the most successful of the wide band models", with errors of up to +/- 20% when compared with empirical data. Therefore, the Exponential Wide Band Model will be used to calculate the emissivity of the plume for use in the equation:

$$E = \varepsilon \sigma T_e^4 \qquad [\text{W/m}^2\text{-sr}] \qquad (32)$$

where E is the emissive power of the plume, ε is the emissivity, σ is the Stefan-Boltzmann constant and T_e is the plume temperature. The radiant intensity of the plume can be determined from

$$I = \frac{E}{\pi} \qquad [\text{W/m}^2\text{-sr}] \qquad (33)$$

where I is the radiant intensity of the plume. The equations used to calculate emissivity are as follows:

The band width parameter

$$\omega = \omega_o \sqrt{\frac{T_e}{T_o}} \qquad (34)$$

The band overlap parameter

$$\gamma = \gamma_o \left(\frac{\gamma}{\gamma_o} \right) \qquad (35)$$

where the term in parenthesis is taken from Figures [21] and [22], for H_2O and CO_2 respectively.
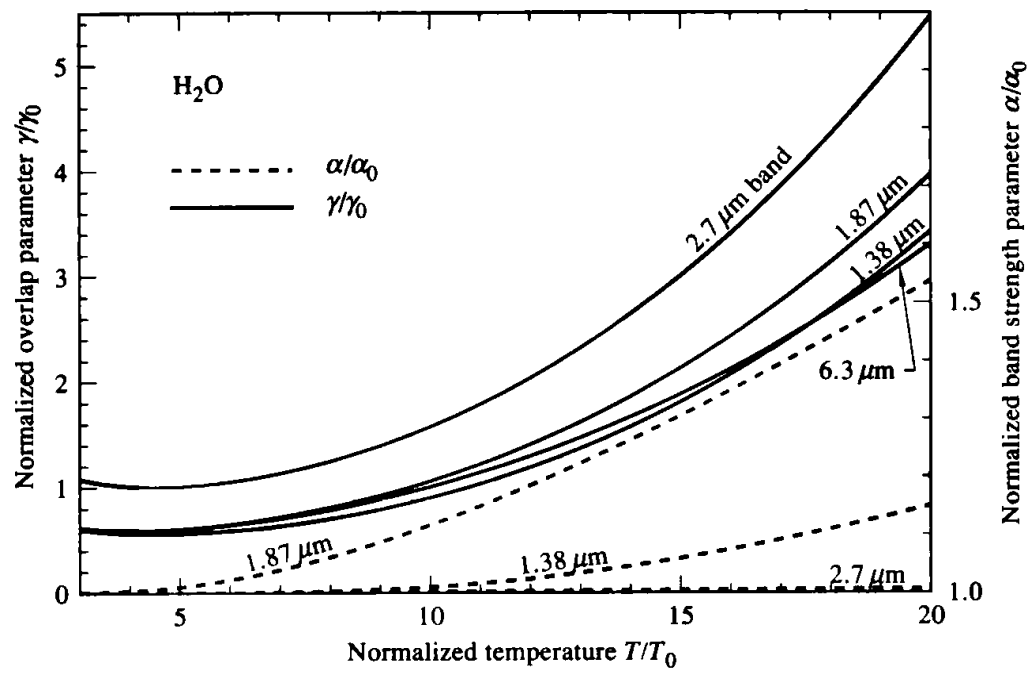
Figure 21 Temperature Dependence of the line overlap parameter, γ, and band strength parameter, α, for water vapor, from Reference [13].
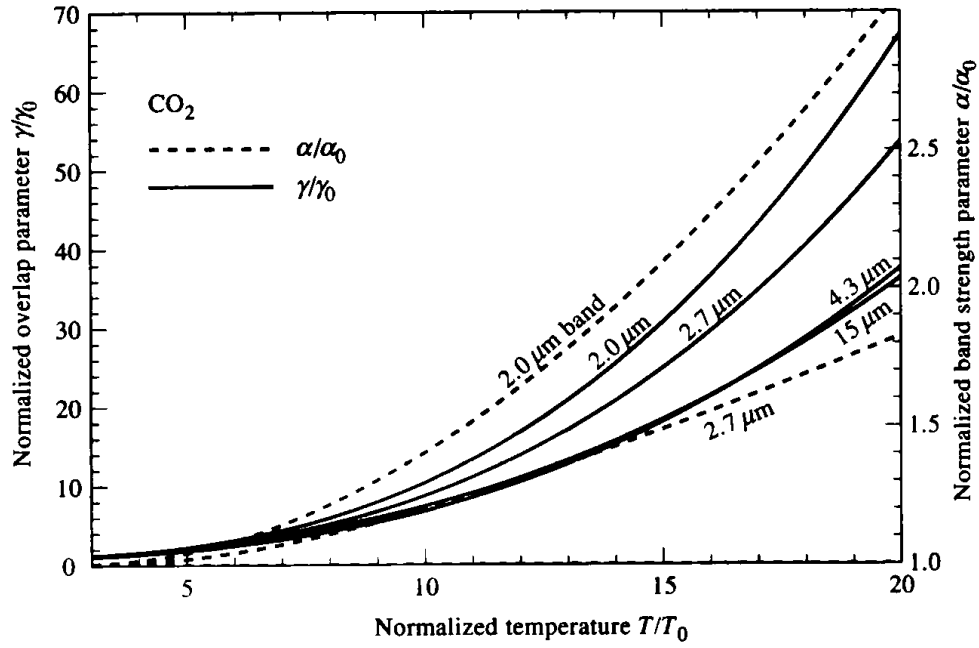
Figure 22 Temperature dependence of the line overlap parameter, γ, and band strength parameter, α, for carbon dioxide, from Reference [13].

The effective pressure is given by

$$P_e = \left[\frac{p}{p_o}\left(1+(b-1)\frac{p_a}{p}\right)\right]^n \tag{36}$$

where p_o is 1 atm, p_a is the total pressure of the plume and p is the partial pressure of the gas, either CO_2 or H_2O. The line overlap parameter, β is given by

$$\beta = \gamma P_e \tag{37}$$

The pressure path length is

$$X = \rho_a s \tag{38}$$

where s is the path length through the plume as shown in Figure [24] and ρ_a is the density of the absorbing gas. The gas band optical thickness is given by

$$\tau_o = \frac{\alpha_o X}{\omega} \tag{39}$$

38

The non-dimensional band absorbtance, A*, can now be determined from the following table:

TABLE 9.2
Exponential wide band correlation for an isothermal gas

$\beta \leq 1$	$0 \leq \tau_0 \leq \beta$	$A^* = \tau_0$	Linear regime
	$\beta \leq \tau_0 \leq 1/\beta$	$A^* = 2\sqrt{\tau_0\beta} - \beta$	Square root regime
	$1/\beta \leq \tau_0 < \infty$	$A^* = \ln(\tau_0\beta) + 2 - \beta$	Logarithmic regime
$\beta \geq 1$	$0 \leq \tau_0 \leq 1$	$A^* = \tau_0$	Linear regime
	$1 \leq \tau_0 < \infty$	$A^* = \ln\tau_0 + 1$	Logarithmic regime

α, β, and ω from Table 9.3 and equations (9.69) through (9.76), $\tau_0 = \alpha X/\omega$.

Figure 23 Exponential wide band correlation for an isothermal gas, from Reference [13].

For each of the preceding equations, the correlation parameters of n, b, α_0, γ_0 and ω_0 are all taken from table 9.3 of reference [13].

The total band absorbtance is then calculated from

$$A = A^*\omega \tag{40}$$

Finally, the emissivity is given by

$$\varepsilon = \left(\frac{E_{b\eta}}{T^3}\right)\left(\frac{A}{T_e}\right) \tag{41}$$

Where $\left(\dfrac{E_{b\eta}}{T^3}\right)$ is found by interpolation of $\left(\dfrac{\eta}{T_e}\right)$ in Appendix C of reference [12].

The preceding equations were written into a MATLAB code to assist in making the calculations. The code was verified by using Example 9-6 in Modest [13]. The values calculated in by the code were identical to those found in Example 9-6 therefore, the code was used for the study. A copy of the code is contained in Appendix E.
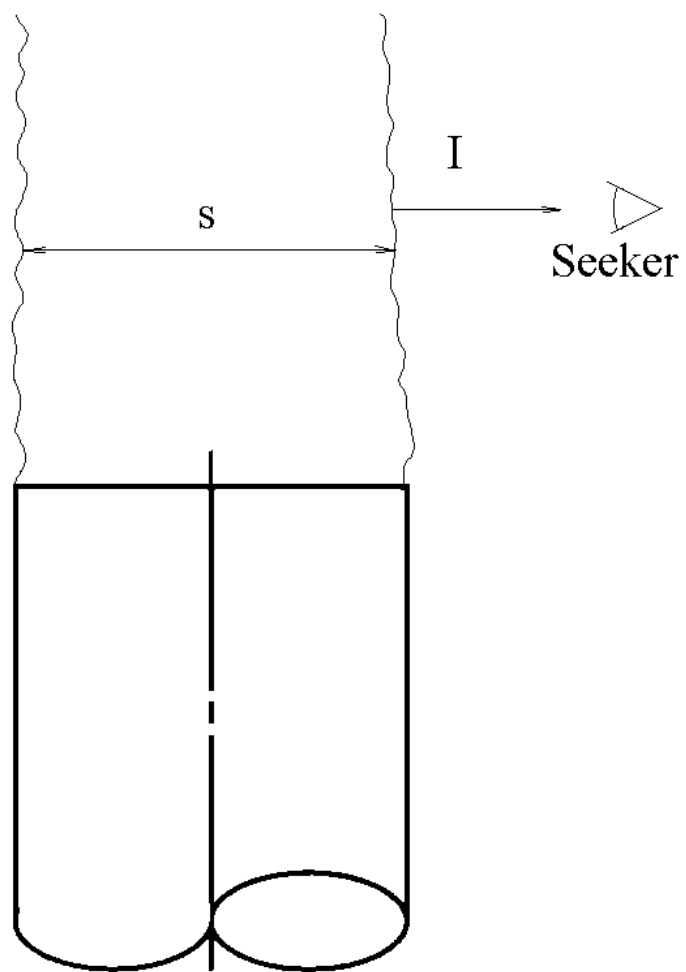
Figure 24 Schematic describing path length.

C.   PLUME INTESITY VERSUS PATH LENGTH

Using the code described in the previous section, the plume's radiant intensity was estimated for various aspect ratios of the same cross-sectional area. The first step was to determine the fuel-to-air ratio, for this study performance data for the LM2500 at full power was used. Based on an exhaust mass flow rate of $\dot{m}_{exhaust}$ = 153 lbm/s and specific fuel consumption, SFC, of 0.37 lbm/hp-hr, the fuel-to-air ratio could be determined from the following equations:

$$f = \frac{\dot{m}_{fuel}}{\dot{m}_{air}} \qquad (42)$$

$$\dot{m}_{fuel} = SFC * P_s \quad \text{where } P_s = 32{,}000 \text{ hp} \qquad (43)$$

$$\dot{m}_{fuel} + \dot{m}_{air} = \dot{m}_{exhaust} \qquad (44)$$

The resultant fuel-to-air ratio was 0.0224.

The next step was to determine the proper stoichiometry for complete combustion. Assuming there was no excess air used in the combustion process, the balanced reaction would be

$$C_{10}H_{19.185} + 14.8O_2 + 67.7N_2 -> 10CO_2 + 9.59H_2O + 24O_2 + 67.7N_2 \qquad (45)$$
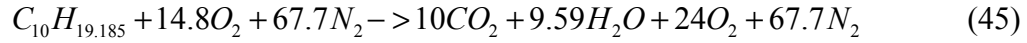
Since the LM2500 requires 44.6 lbm of air for every lbm of fuel burned, and assuming air is 20% O_2 and 80% N_2, the amount of excess air used in the actual combustion process can be determined. The excess air can then be added to the combustion process in Equation (45) resulting in the following stoichiometric reaction

$$C_{10}H_{19.185} + 38.8O_2 + 177.5N_2 -> 10CO_2 + 9.59H_2O + 24O_2 + 177.5N_2 \qquad (46)$$
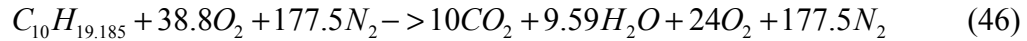
Where the partial pressures of the exhaust gases can be determined from the mole fractions as follows

$$p_{gas} = \frac{\#moles_{gas}}{\#moles_{total}}(1atm) \qquad (46)$$

The partial pressures of CO_2 and H_2O are 5% and 5% respectively. The partial pressures and temperature of the plume were then entered into the code to determine the radiant intensity of the plume.

The first path length, s, was that of the current DDG 51 geometry where the path length was through the plume axis. The circular cross-section was then converted to a square of the same area. Next the aspect ratio (AR) was varied from 1:1 to 40:1. The minor axis was the path length of interest, Figure [25], as it was assumed that the exhaust system would be oriented in such a way as to present the minimum path length to an incoming missile.
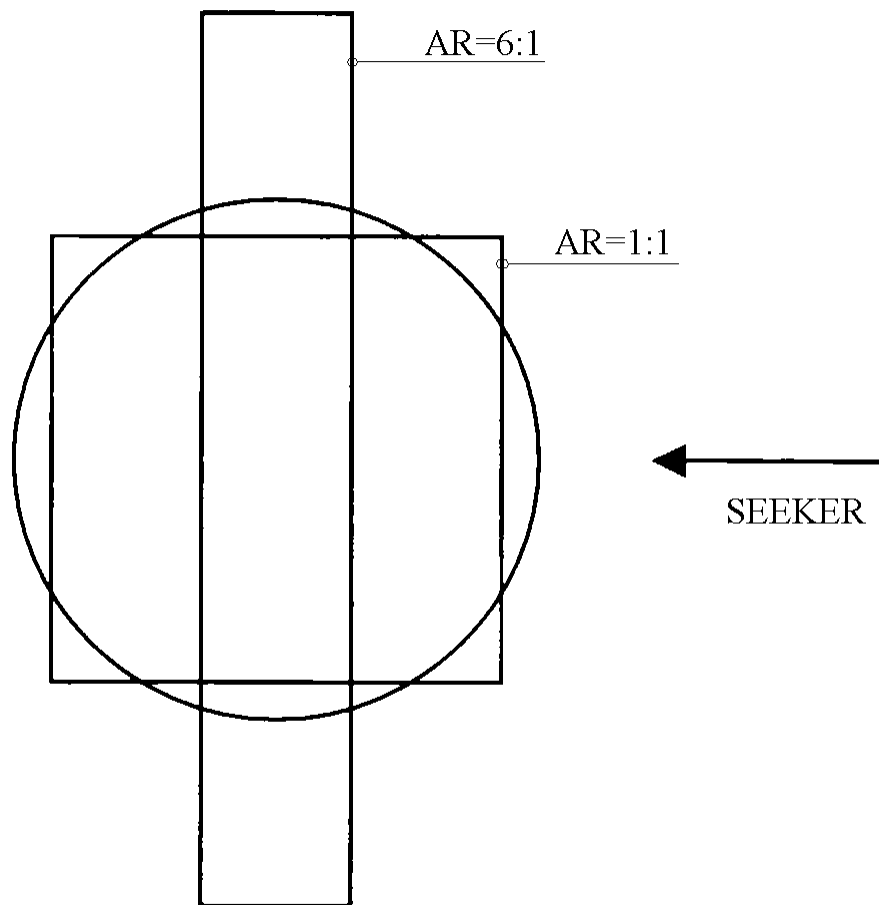
Figure 25 Plan view illustrating exhaust orientation to IR Seeker.

The study revealed, as expected, that the radiant intensity of the plume decreases as path length decreases. Figure [26] illustrates the dependence of plume intensity on path length for a cooled and uncooled plume, while Figures [27] and [28] show the emissivities of the individual gas at the specified wavelength. Based on the following graphs, the radiant intensity of the cooled exhaust can be reduced to one-eighth that of the uncooled plume for the circular cross-section. If the total gas emissivities for the cooled and uncooled plume were equal, it would be expected that $I_{cooled} = 1/16 I_{uncooled}$ since the temperature of the cooled exhaust is nearly half that of the uncooled, as given by $T_{uncooled} = 2T_{cooled}$ and $I_{cooled} = \varepsilon_{cooled} \sigma T_{cooled}^4$. However, the total gas emissivities are not equal. Figures [27 d] and [28 d] show that the total gas emissivity of the uncooled plume is slightly more than double that of the cooled plume, so that $I_{cooled} = 1/8 I_{uncooled}$.
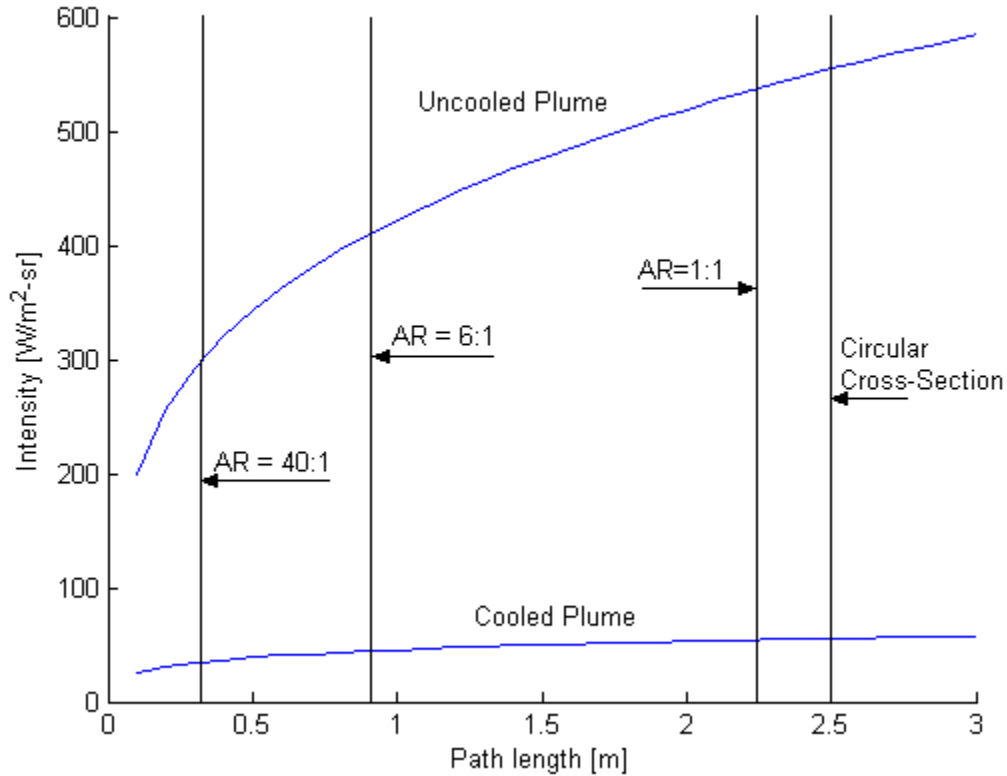
Figure 26 Total radiation intensity versus path length of a plume.
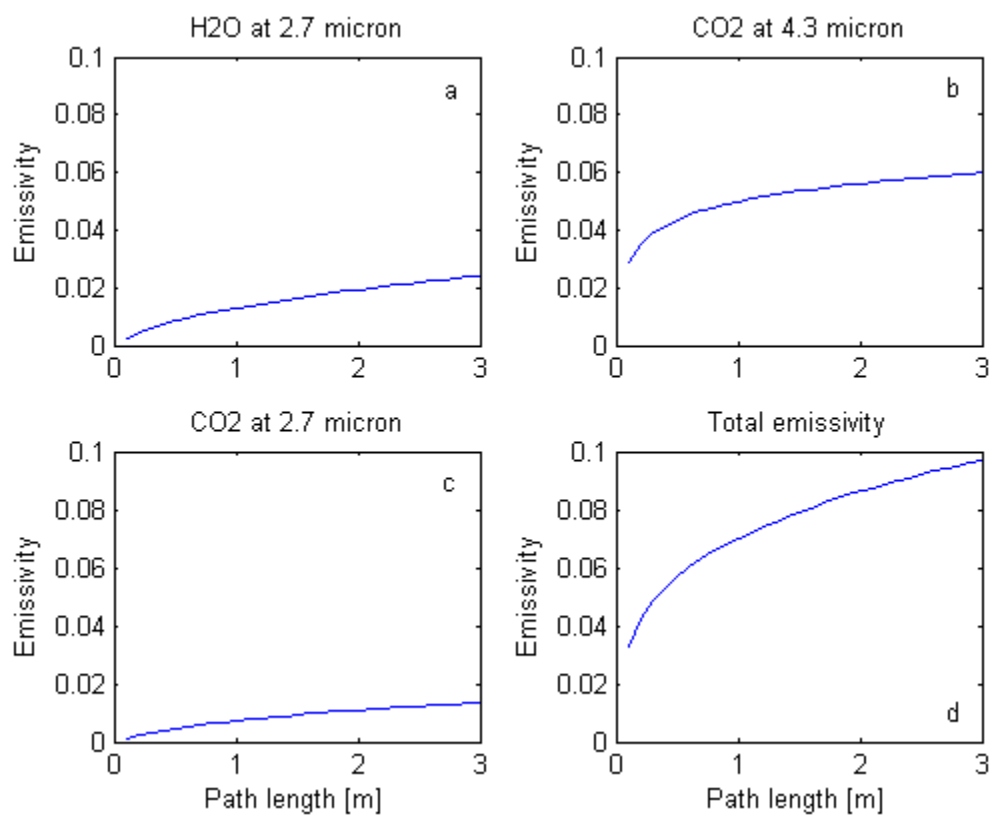
Figure 27 Gas emissivity versus path length for each spectral band (uncooled plume at 5% CO_2 and 5% H_2O).
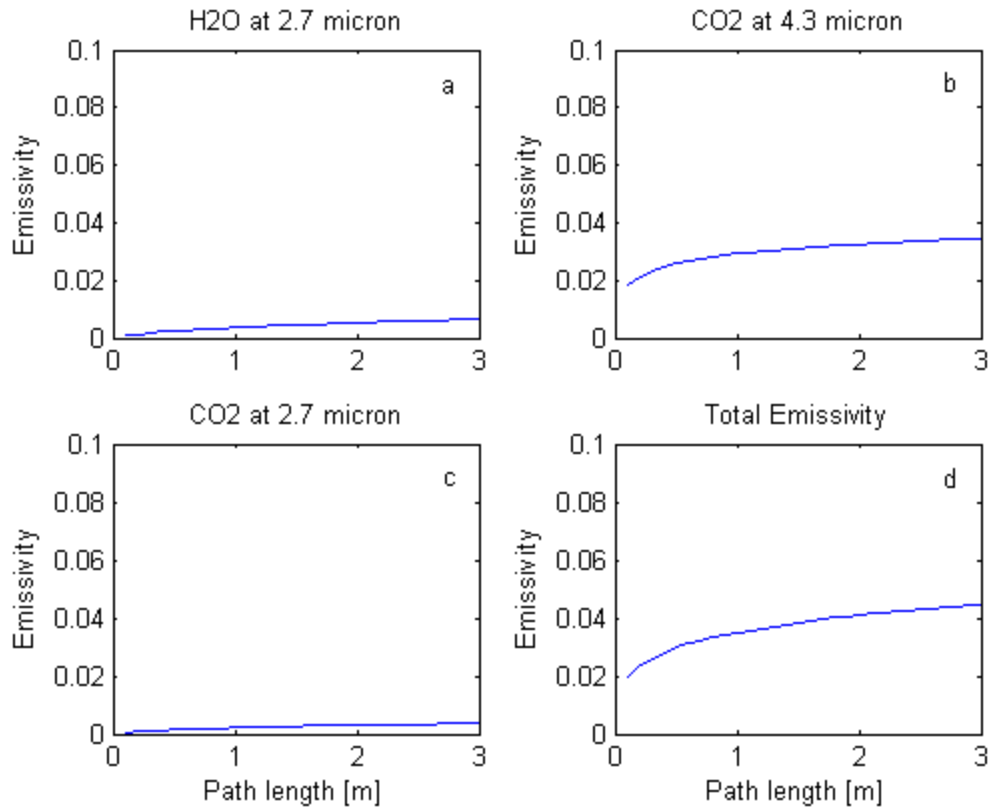
Figure 28 Gas emissivity versus path length for each spectral band (cooled plume at 5% CO_2 and 5% H_2O).

The preceding graphs show that cooling the plume significantly reduces its infrared signature, and converting the exit geometry from a circular cross-section to a long thin rectangle can reduce the radiant intensity of the plume. Figure [29] shows that for a cooled plume, the radiant intensity can be reduced by 40% if a 40:1 aspect ratio slot were used in place of a circular cross-section, this would result in a slot that is approximately 40 ft by 1 ft for DDG 51. In comparison, a more reasonable aspect ratio of 6:1 results in a 20% reduction in plume intensity. Again, the results of this study are based on the assumption that the plume is isothermal and homogeneous. Based on the results of the study, the shipbuilder must be willing to compromise between the possible loss of topside space and weight gain in order to reduce the radiant intensity of the plume a significant amount.
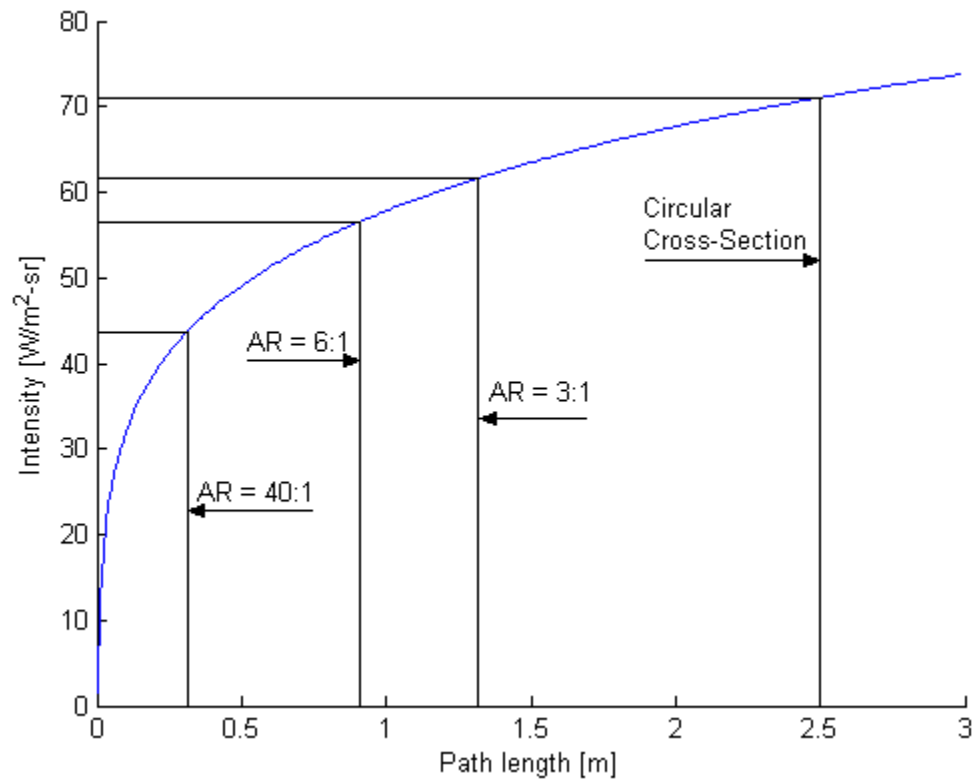
Figure 29 Total gas intensity versus path length for cooled plume showing various aspect ratios and corresponding intensities.

VI. SUMMARY AND CONCLUSIONS

A. SUMMARY

A one-dimensional model of an enhanced mixing eductor system was developed and used to predict exhaust temperature, secondary air mass flow rate and backpressure. The predictions obtained from the model were then used to determine the preliminary design of a gas turbine exhaust system for the LHA (R) program. The design included an oval-to-rectangular transition duct. The geometry of the transition was determined using a super-ellipse and the total pressure losses within the transition were determined from empirical data taken from a similar duct design. The duct losses were included in the exhaust system model to enhance the predictions. A lobed nozzle was selected for the design in order to reduce the mixing tube length. Additionally, a code was written, that used an Exponential Wide Band Model to study the effect of path length on exhaust plume radiant intensity, and showed that changing the aspect ratio of the mixing tube exit plane can further reduce the plume's infrared signature.

B. CONCLUSIONS

The following conclusions were obtained:

1. An enhanced mixing eductor system that fits within the existing framework of the LHA (R) uptake space was designed. The proposed system provides a 46% reduction in exhaust temperature, an improvement of 10% compared to DDG 51.

2. An estimate of the proposed system backpressure was calculated and compared with an uncooled system. The increase in backpressure developed by the eductor system was approximately 6 "H_2O which is within the limit of the engine. Additionally, an oval-to-rectangular transition geometry was provided. The estimated total pressure loss coefficient for the transition was estimated to be 0.2.

3. The radiant intensity of the plume can be reduced greater than 40% for slotted mixing tube geometries with an aspect ratio of greater than 40:1. However, due to space and weight constraints a more realistic reduction in signature of up to 20% can be achieved for an aspect ratio of 6:1.

LIST OF REFERENCES

1. Dalton, T., Boughner, A., Mako, C. D., Doerry, N., "*LHD 8: A Step Toward the All Electric Warship*", Presented at ASNE Day 2001, Arlington, Va, 30 April-1 May 2001

2. Wilsted, H. D., Huddleston, S. C., Ellis, C. W., 1949, "*Effect of temperature on performance of several ejector configurations*", NACA Research Memorandum, RM E9E16, June 1949.

3. Hussmann, A. W., 1953, "*Ventilation eductors in gas turbine exhaust stacks*", USN Bureau of Ships, Index No. NS 622-078, May 1953.

4. Ellin, C. R., "*Model tests of multiple nozzle gas eductor systems for gas turbine powered ships*", Engineer's Thesis, Naval Postgraduate School, Monterey, CA, June 1977.

5. Presz, W. M., Blinn, R. F., Morin, B., 1987, "*Short Efficient Ejector Systems*", AIAA Paper Number 87-1837.

6. Otis, R. H., "*Preliminary Design Study for an Enhanced Mixing Eductor for Gas Turbine Exhaust Systems*", Master's Thesis, Restricted Distribution, Naval Postgraduate School, March 1998.

7. "*LM2500 Marine Gas Turbine Installation Design Manual*", General Electric Marine & Industrial Engines, MID-TD-2500-2, Revised December 1990.

8. Keenan, J. H., Neumann, E. P., 1942, "*A Simple Air Ejector*", Journal of Applied Mechanics, June 1942.

9. Nichols, G., Tripp, S., "*LM2500/DDG-51 Full Scale Air Intake and Exhaust System Test Results and Evaluation for the No. 2 Engine Room Outboard Engine*", General Electric, Evendale Technical Information Center, February 1991.

10. Idelchik, I. E., "*Handbook of Hydraulic Resistance*", Hemisphere Publishing Corporation, Second Edition, 1986.

11. Patrick, W. P., McCormick, D. C., "*Laser Velocimeter and Total Pressure Measurements in Circular-to-Rectangular Transition Ducts*", United Technologies Research Center, Report Number UTRC87-41, June 1988.

12. White, F. M., "*Fluid Mechanics*", McGraw Hill, Fourth Edition, 1999.

13. Modest, M. F., "*Radiative Heat Transfer*", McGraw Hill, 1993.

14. Incropera, F. P., DeWitt, D. P., "*Introduction to Heat Transfer*", John Wiley and Sons, Fourth Edition, 2002.

15. Birk, A. M., VanDam, D., "*Marine Gas Turbine Infra-Red Signature Suppression: Aerothermal Design Considerations*", ASME Report Number 89-GT-240, June 1989.

16. General Electric Aircraft Engines website, Last accessed 1 December 2003. http://www.geae.com/engines/marine/lm2500+.html,

APPENDIX A

1-D CORRECTED MODEL

{Thesis Project: LHA(R) Exhaust Design Study}
{Written by Steve Dudar, MSME Dec 03}
{See Figure [7] for clarification of symbology}

{CONSTANTS}
{Gas constant R [J/kg-K], assumed exhaust gases were air}
R=287

{Specific heat ratio (assumed constant), gamma=Cp/Cv}
gamma=1.4

{Acceleration due to gravity [m/s^2]}
g=9.81

{Density of fresh water [kg/m^3]}
rho_h2o=1000

{Assumed ISO-STP at sea level, T [K], P [Pa]}
T_amb=288
P_amb=101325
{P_4=P_amb}
{Friction factor, for new stainless steel}
f=0.01

{PRIMARY FLOW at entrance}
{From LM-2500+ technical data at given conditions}

{CONTROL VOLUME 1}
{Exhaust mass flow at turbine exit [kg/s]}
m_dot_a=94.8
m_dot_a=rho_a*A_a*V_a

{Exhaust temperature at turbine exit [K]}
T_a=760

{Stack cross-sectional area [m^2]}
A_a=3.6
{A_1=A_a}

{Hydraulic diameter [m]}
D_ha=1.95

{Height of section 1 [m]}
Z_a=24.6
Z_1=36.3

{Equations of state}
P_a=rho_a*R*T_a
P_1=rho_a*R*T_1

{Continuity}
m_dot_a=m_dot_1
m_dot_1=rho_a*A_1*V_1

{Bernoulli's equation at entrance}
P_ta=P_a+0.5*rho_a*V_a^2
P_t1=P_1+0.5*rho_a*V_1^2

{Energy equation}
P_a/(rho_a*g)+(V_a^2)/(g*2)+Z_a=P_1/(rho_a*g)+(V_1^2)/(2*g)+Z_1+H_f1
H_f1=f*((Z_1-Z_a)/D_ha)*(V_a^2)/(2*g)
H_1air=H_f1
SG_1=rho_a/rho_h2o
H_1h2o=H_1air*SG_1/0.3048*12   {[inches H2O]}

{CONTROL VOLUME 2}
{Cross sectional area [m^2] at transition exit plane}
A_2=3.37

{Height of section 2}
Z_2=39.32

{Equation of state}
P_2=rho_a*R*T_2

{Continuity}
m_dot_2=m_dot_a
m_dot_2=rho_a*A_2*V_2

{Energy equation}
P_1/(rho_a*g)+(V_1^2)/(g*2)+Z_1=P_2/(rho_a*g)+(V_2^2)/(2*g)+Z_2+H_f2

zeta_t=0.2   {Minor loss coefficient for transition duct}
H_f2=zeta_t*(V_2^2)/(2*g)
H_2air=H_f2
H_2h2o=H_2air*SG_1/0.3048*12   {[inches H2O]}

{CONTROL VOLUME 3}
{Cross sectional area at nozzle exit plane}
{A_3=2.276 } {VARIABLE}

{Height of section 3}
Z_3=40.54

{Equation of state}
P_3=rho_a*R*T_3

{Continuity}
m_dot_3=m_dot_a
m_dot_3=rho_a*A_3*V_3

{Energy equation}
P_2/(rho_a*g)+(V_2^2)/(g*2)+Z_2=P_3/(rho_a*g)+(V_3^2)/(2*g)+Z_3+H_f3

zeta_n=0.1   {Minor loss coefficient for nozzle}
H_f3=zeta_n*((V_3^2)/(2*g))
H_3air=H_f3+((V_3^2)/(2*g))
H_3h2o=H_3air*SG_1/0.3048*12   {[inches H2O]}

A_1=A_a

{SECONDARY FLOW}
{Assume that secondary flow is air at ISO-STP}
T_4=T_amb
P_t4=P_amb
P_4=P_3

{Secondary air mass flow [kg/s]}
m_dot_4=rho_4*A_4*V_4

{BERNOULLI'S EQUATION AT THE MIXING TUBE INLET}
P_t4=P_4+(0.5*rho_4*(V_4^2))

{Equation of state}
P_4=rho_4*R*T_4

{TERTIARY FLOW}
{Assume Pe=Pamb}
P_e=P_amb
m_dot_e=rho_e*A_e*V_e
A_e=(A_3+A_4)
P_e=rho_e*R*T_e

A_e=7

{continuity}
m_dot_a+m_dot_4=m_dot_e

{Momentum equation}
m_dot_e*V_e-m_dot_3*V_3-m_dot_4*V_4=P_3*A_3+P_4*A_4-P_e*A_e

{Energy equation}
m_dot_3*((gamma/(gamma-1))*R*T_3+0.5*V_3^2)+m_dot_4*((gamma/(gamma-1))*R*T_4+0.5*V_4^2)=m_dot_e*((gamma/(gamma-1))*R*T_e+0.5*V_e^2)

{STATIC BACK PRESSURES}
DELTAP =P_ta-P_3

{Pumping ratio}
W=m_dot_4/m_dot_a

{Mass flow correction}
m_dot_4_real=0.8*m_dot_4
m_dot_4_real=rho_4*A_4*V_4_real
W_real=m_dot_4_real/m_dot_a
m_dot_e_real=m_dot_a+m_dot_4_real
m_dot_e_real=rho_e*A_e*V_e_real

{Momentum equation}
m_dot_e_real*V_e_real-m_dot_3*V_3-
m_dot_4_real*V_4_real=P_3*A_3+P_4_real*A_4-P_e*A_e

{Energy equation}
m_dot_3*((gamma/(gamma-1))*R*T_3+0.5*V_a^2)+m_dot_4_real*((gamma/(gamma-1))*R*T_4+0.5*V_4_real^2)=m_dot_e_real*((gamma/(gamma-1))*R*T_e_real+0.5*V_e_real^2)

APPENDIX B

DIESEL EXHAUST DESIGN STUDY

Since the diesel exhaust had to be rearranged in order to accommodate the proposed gas turbine exhaust eductor system, it was decided to propose a similar eductor system for the diesel exhaust. Following the same methodology as described in chapter III, and using the parameters for a Colt-Pielstick PA6 diesel engine operating at full power, nozzle exit area was determined. It was not necessary to determine the mixing tube exit area using the code since the area was constrained by the gas turbine exhaust mixing tube. Figure [25] shows backpressure and exit temperature versus nozzle exit area. In order to determine the backpressure placed on the engine due to the eductor system, a nozzle loss coefficient and "S" duct loss coefficient of 0.1 and 0.2, respectively was assumed. The resultant exit temperature was reduced by 30% with an increase of 2 in H_2O, as compared to the uncooled diesel exhaust.
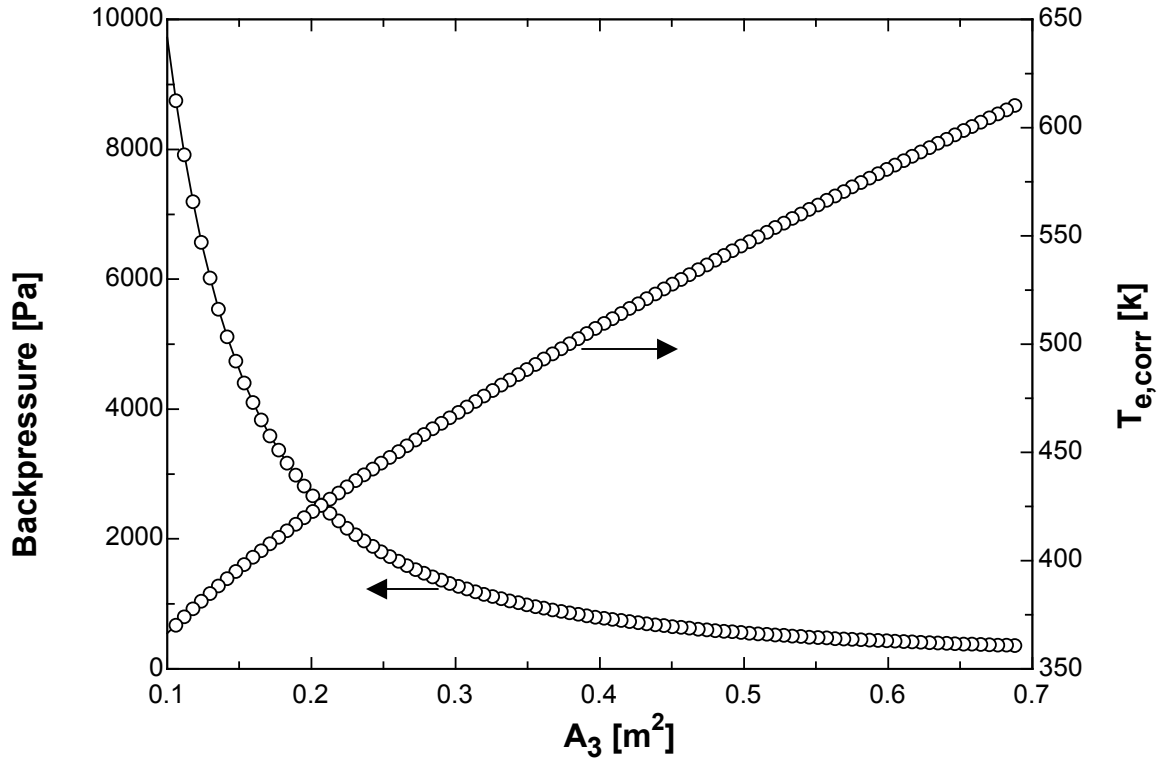

Figure 30 Backpressure and exit temperature versus nozzle exit area (SSDG).

THIS PAGE INTENTIONALLY LEFT BLANK

APPENDIX C

TRANSITION DUCT DESIGN

Coefficients for transition duct super-ellipse, equation (28)

X [ft]	a [ft]	b [ft]	c [ft]	nz	my
0.0000	4.7900	2.2500	0.0000	3.0000	0.3333
0.5000	4.9130	2.1938	0.1230	3.1250	0.3200
1.0000	5.0360	2.1375	0.2460	3.2500	0.3077
1.5000	5.1590	2.0813	0.3690	3.2500	0.3077
2.0000	5.2820	2.0250	0.4920	3.5000	0.2857
2.5000	5.4050	1.9688	0.6150	3.7500	0.2667
3.0000	5.5280	1.9125	0.7380	4.0000	0.2500
3.5000	5.6510	1.8563	0.8610	4.2500	0.2353
4.0000	5.7740	1.8000	0.9840	4.5000	0.2222
4.5000	5.8970	1.7438	1.1070	5.0000	0.2000
5.0000	6.0200	1.6875	1.2300	5.5000	0.1818
5.5000	6.1430	1.6313	1.3530	6.0000	0.1667
6.0000	6.2660	1.5750	1.4760	7.0000	0.1429
6.5000	6.3890	1.5188	1.5990	8.0000	0.1250
7.0000	6.5120	1.4625	1.7220	9.0000	0.1111
7.5000	6.6350	1.4063	1.8450	10.0000	0.1000
8.0000	6.7580	1.3500	1.9680	10.0000	0.1000
8.5000	6.8810	1.2938	2.0910	10.0000	0.1000
9.0000	7.0040	1.2375	2.2140	10.0000	0.1000
9.5000	7.1270	1.1813	2.3370	10.0000	0.1000
10.0000	7.2500	1.1250	2.4600	10.0000	0.1000

Transition Duct MATLAB code:

% This code calculates the geometry of an oval-to-rectangular transition duct.

% The code only calculates one half the geometry about the plane of symmetry (x axis).

% Written by S. W. Dudar

```
x=zeros(21);
for i=2:22
    x=x+0.5;
    z=0:b(i-1)/20:b(i-1);
    y=a(i-1)*((1-(z.^nz(i-1))/b(i-1)^nz(i-1)).^ny(i-1))+c(i-1);
    y1=-y+2*c(i-1);
    plot3(x,y,z,x,y,z,x,y,-z,x,y,-z);
    hold on
end
```

APPENDIX D

TRANSITION DUCT TOTAL PRESSURE LOSS COEFFICIENT MATLAB CODE

```
% This MATLAB code was used to determine the Total Pressure loss coefficient in the

% AR630 transition duct, Ref [10].

% Written by S. W. Dudar

clear all

% Create AR630 inlet velocity profile

ra=1;

rb=1;

nz=10;

ny=1/nz;

dr=0:rb/500:rb;

r_R=dr;

U1_Uref=ra.*((1-(r_R.^nz)./rb.^nz).^ny);

r_R2=-r_R;

dTheta=0:2*pi/500:2*pi;

% Determine inlet Total Pressure

Pref=14.7;                              %{[Psia]}

Uref=100;                              %{[ft/s]}

rho=0.06762;                           %{[lbm/ft^3]}

Qref=0.5*rho/32.2*Uref^2;              %{[Psia]}

U1=U1_Uref*Uref;

k1=U1_Uref;

Pt1=k1.*Qref/144+Pref;                 %{[Psia]}

Pm1=0;

mdot1=0;

for i=1:501

   for j=1:501

      Pm1=Pt1(j)*U1(j)*r_R(i)*dr(j)*dTheta(i)+Pm1;

      mdot1=U1(j)*r_R(i)*dr(j)*dTheta(i)+mdot1;
```

```matlab
    end
end
PT1=Pm1/mdot1
% Determine exit Total Pressure
k2=xlsread('loss data','dP_Qref');
U2_Uref=xlsread('loss data','u_Uref');
dy=xlsread('loss data','dy')';
dz=xlsread('loss data','dz')';
Pt2=k2.*Qref/144+Pref;
U2=U2_Uref*Uref;
Pm2=0;
mdot2=0;
for i=1:11
   for j=1:11
      Pm2=Pt2(i,j)*U2(i,j)*dy(i)*dz(j)+Pm2;
      mdot2=U2(i,j)*dy(i)*dz(j)+mdot2;
   end
end
PT2=Pm2/mdot2
% Determine Total Pressure Loss Coefficient
K=144*(PT1-PT2)/Qref
```

APPENDIX E

EXPONENTIAL WIDE BAND MODEL CODE

```
%{CONSTANTS}
T_0=100;                          %{[K]}
p_0=1;                            %{[atm]}
p=1;                             %{[atm]}
sigma=5.67e-8;                   %{Stefan-Boltzmann constant}

Y=xlsread('Black Body Emissivity','Sheet2');
x=xlsread('Black Body Emissivity','Sheet1');

% {VARIABLES}
T_e={user input};                %{Exit Temperature [K]}
p={user input};                  %{Gas partial Pressure [atm]}
s={variable};                    %{Path length [m]}




% {From Table 9.3 Modest [12]}
eta=;                            %{[1/cm]}
n=;
b=;
alpha_0=;                        %{[m^2/(cm*g)]}
gamma_0=;
omega_0=;                        %{[1/cm]}
L=eta/T_e;                       %{[1/(cm*K)]}

omega=omega_0*sqrt(T_e/T_0);
gamma=gamma_0*2;
P_e=((p/p_0)*(1+(b-1)*(p_a/p)))^n;
beta=gamma*P_e
rho_a=44*(1000/22.4)*(273/T_e)*p;

for i=1:length(s)
       X(i)=rho_a*s(i);
       tau(i)=alpha_0*X(i)/omega

       while beta <= 1
              if (tau(i) <= beta) & (tau(i) >= 0)
                     A1(i) = tau(i);
                     break
              elseif (tau(i) <= 1/beta) & (tau(i) >= beta)
                     A1(i) = 2*sqrt(tau(i)*beta2)-beta2;
                     break
```

61

```
            elseif (tau(i) < 1e6) & (tau(i) >= 1/beta)
                    A1(i) = log(tau(i)*beta)+2-beta2;
                    break
            end
            break
    end

    while beta >= 1
            if (tau_co2(i) <= 1) & (tau(i) >= 0)
                    A1(i) = tau(i);
                     break
            elseif (tau_co2(i) < 1e6) & (tau(i) >= 1)
                    A1(i) = log(tau(i))+1;
                    break
            end
            break
    end

    A=A1(i)
    A(i) = A1(i)*omega;

    Mi = interp1(Y,x,L);
    J2(i) = Mi *A(i);
    epsilon(i) = J2(i)/(sigma*T_e);

    I (i)=(epsilon (i)*sigma*T_e^4)/pi;

end

hold on
plot(s,epsilon)
%plot(s,I)
%plot(s,tau)
hold off
```

INITIAL DISTRIBUTION LIST

1. Defense Technical Information Center
    Ft. Belvoir, VA

2. Dudley Knox Library
    Naval Postgraduate School
    Monterey, CA

3. Department Chairman, Code ME
    Department of Mechanical Engineering
    Naval Postgraduate School
    Monterey, CA

4. Professor Knox T. Millsaps, Jr
    Department of Mechanical Engineering
    Naval Postgraduate School
    Monterey, CA

5. Professor Christopher Brophy
    Department of Mechanical Engineering
    Naval Postgraduate School
    Monterey, CA

6. Curricular Officer, Code 74
    Department of Mechanical Engineering
    Naval Postgraduate School
    Monterey, CA

7. Stephen W. Dudar
    Jacksonville, Fl

8. Mr. Ray Ratcliffe, Code 7230
    NSWC, Carderock Division
    West Bethesda, MD